ESTIMATING TUNNEL DEFORMATION USING A NONLINEAR FINITE ELEMENT PROGRAM

A Practicum

Presented to

The Department of Civil Engineering

The Faculty of Graduate Studies

The University of Manitoba

In Partial Fulfillment

of the Requirements for the Degree

Master of Engineering

by

A. Douglas McAndrew

September 1983

ESTIMATING TUNNEL DEFORMATION USING A NONLINEAR FINITE ELEMENT PROGRAM

by

A. Douglas McAndrew

A practicum submitted to the Faculty of Graduate Studies of the University of Manitoba in partial fulfillment of the requirements of the degree of

MASTER OF ENGINEERING

ACKNOWLEDGEMENTS

The author is grateful to Dr. L. Domaschuk, Associate Head and Professor of Civil Engineering, University of Manitoba, for establishing the topic of this practicum, particularly when it was for a Master of Engineering student. The author would also like to express his appreciation to Mr. E. Yong for his assistance with the finite element program.

Finally, the author is greatly indebted to his parents for their assistance, time, and support during the economic recession which resulted in this higher education.

ABSTRACT

The applicability of a nonlinear load-deformation finite element program, developed at the University of Manitoba, to the problem of estimating the deformations associated with soft ground tunnelling operations in Winnipeg was investigated in this study. By using actual geotechnical data (i.e. - moisture contents, plasticity indecies, etc.) from a closely monitored and well documented tunnel in Winnipeg in the finite element model, it was possible to assess the accuracy and limitations of the program by comparing the computed values with the measured field values.

The model provided very good estimates of deformation at the tunnel wall, however the agreement between predicted and observed deformation at points away from the tunnel wall was poor.

The deformations according to the model approached zero asymptotically with radial distance from the wall, whereas the observed deformations decreased approximately linearly with distance from the tunnel wall.

TABLE OF CONTENTS

INTRODUCTION

Deformations resulting from tunnelling operations in soft ground have been a concern for many years. In todays cluttered urban areas, these deformations not only affect surface structures, but also the multitude of buried services such as gas and water lines. As well, knowledge of the deformations is useful in determining the short and long term stability of the surrounding soil mass and in calculating tunnel support and liner requirements. Consequently, accurate estimates of the magnitude and distribution of these deformations prior to construction, particularly for large diameter tunnels near the ground surface, is essential for safe and economical tunnel design.

At present there are no simple reliable methods for accurately calculating or predicting these deformations. The variables involved are just too numerous to incorporate into a closed-form solution. In recent years the development of numerical methods and various computer techniques such as finite elements, have made it possible to model soft ground tunnelling operations more realistically.

The majority of finite element investigations in soft ground tunnelling (Hardy et al, 1981 ; Hoyaux and Ladanyi, 1969) have used linear analyses and the results were not satisfactory. It is realised that nonlinear analyses offer a better representation of the physical problem (Desai and

Christian, 1977) and therefore yield better solutions. Unfortunately, three problems are generally associated with this technique:

1) Commercially available programs are expensive.
2) The nonlinear model describing the soil behavior is seldom fully understood by the user.
3) The deformation parameters necessary for the analysis are difficult to quantify.

The purpose of this practicum is to investigate the applicability of an inexpensive nonlinear finite element program, developed at the University of Manitoba, to the problem of estimating the deformations associated with soft ground tunnelling operations in the Winnipeg area. This was done by modelling an existing closely monitored and well documented tunnel in the Winnipeg area. Using geotechnical data from the site in the finite element program made it possible to assess the accuracy and limitations of the program by comparing the computed values with the actual values observed in the field.

CHAPTER II

2.0 METHODS OF PREDICTING GROUND MOVEMENTS ASSOCIATED WITH TUNNELLING

The literature contains several studies on tunnel design in soft ground (Muir Wood, 1975; Peck et al, 1972; Henkel, 1970). However the majority are only concerned with estimating stresses around the tunnel. Although useful, this information is only a small part of what is required for a complete tunnel design.

More recently, attention has been given to estimating deformations associated with tunnelling operations in soft ground, which is more useful. From a designer's point of view, knowing the anticipated deformations makes it possible to assess the short and long term stability of the surrounding soil mass; to calculate support and liner requirements; and to specify construction practices. From a contractor's point of view, stresses are meaningless as they are not visible, only their effects are; namely strains, distortions, displacements, and ground surface settlements. Consequently, if these deformations can be predicted accurately in advance of the excavation, better all-round tunnel design and operations can be effected.

2.1 EMPIRICAL METHODS

Empirical techniques for predicting ground movements are

not very common in the literature. Clough and Schmidt, 1981 cite the major reason for this as being the complexity of the deformations associated with tunnelling. Displacements at the tunnel face are three dimensional, moving both axially toward the advancing tunnel and radially toward the tunnel walls. The authors suggest that for an order of magnitude assessment of probable displacements this complexity may be ignored, and it can be assumed that the tunnel is excavated instantaneously such that displacements are only radial. With this in mind, an empirical solution for calculating the loss of ground is presented from which an approximate ground settlement curve can be made. The solution is based on the theoretical tunnel dimensions and the actual volume of soil removed, as calculated by summing the theoretical displacements around the periphery resulting from the stress reduction. The solution assumes elastic conditions prevail in the soil and zero volume change in the plastic zone.

Rowe and Kack (1983), suggest the best summary of empirical solutions is contained in a paper by Peck (1969). The authors feel these solutions when applied with appropriate judgement, may yield quite adequate and economical designs. However, it is emphasised that empirical solutions are subject to some important limitations; first, the limited information on the distribution of deformations throughout the entire soil mass; second, their applicability to different tunnel geome-

tries and construction techniques; and third, the consistency of the results.

2.2 NUMERICAL METHODS

Recent advances in theoretical solutions using numerical methods, such as finite elements, have indicated a potential for estimating deformations due to tunnelling, yet their application is still quite limited (Row, Lo, and Kack, 1983). The finite element method has made it possible to overcome the complex boundary conditions, nonhomogeneity, anisotropy, and nonlinearity typical of many geotechnical problems. Unfortunately, our ability to incorporate the appropriate stress-strain characteristics of the soil has not progressed sufficiently.

2.2.1 Linear Analyses

Earlier studies (Hoyaux and Ladanyi, 1969; Ghaboussi, 1978; Tan and Clough, 1980; Hardy et al, 1981) using linear finite element analyses to predict soil movements due to tunnelling in soft ground have displayed promising results in some instances. It is generally agreed however, that there has been insufficient consideration given to the general theoretical and practical factors necessary for these techniques to yield consistently good results. To illustrate this point, the 'reasonable' correlation between field observations and computer analyses described in several of the studies were attained only after revising the elastic parameters (Hardy et al, 1981).

Clearly this technique of revising parameters can not be used in a design office to predict deformations.

2.2.2 Nonlinear Analyses

Rowe and Kack (1983) describe a theoretically based design procedure suitable for different soil types, construction methods, geometries, etc. using an elasto-plastic finite element program. In an earlier paper (forming part of a series on soft ground tunnelling), Rowe, Lo, and Kack (1983) describe the technique used in their study, and illustate it with a comprehensive parametric study. The analyses were performed using a plane strain elasto-plastic finite element program (EPTUN) developed by the authors. The plastic behavior was modelled using a Coulomb-Mohr failure criterion and a nonassociated flow rule. The constitutive equations made use of Young's Modulus and Poisson's Ratio. Assumptions in the analyses included no dilatency for soft or loose soils, and an isotropic drained response of the soil.

Based on four case histories, the authors felt their theory provided reasonable predictions of ground movement, prior to construction, in most cases, requiring only a limited knowledge of the soil profile, tunnel characteristics, and construction methods. However, the authors emphasize that there are certain situations where the proposed theory and current empirical approaches would not provide satisfactory estimates; specifically in circumstances where large volume changes within the soil are possible.

CHAPTER III

3.0 PROPOSED METHOD

As described in Chapter II, the finite element method is a recognised and trusted technique in geotechnical engineering. The problem in its use is incorporating the appropriate geotechnical stress-strain or deformation characteristics of the soil, as it is difficult to evaluate the insitu characteristics from laboratory testing.

The deformation characteristics of an isotropic homogeneous elastic solid can be described by two parameters. These can be Young's Modulus (E) and Poisson's Ratio (ν), the Bulk Modulus (K) and the Shear Modulus (G), or Lame's Constants. Most studies have attempted to use non-constant Young's Modulus derived from standard triaxial compression tests to describe nonlinear behaviour (Hoyaux & Ladanyi, 1969). However, the relationship between the principal stress difference (q) and axial strain (ε_1) in the standard triaxial test does not represent the true deformation characteristics of a soil. The method only considers the change in major principal stress and does not reflect the overall stress conditions in the soil. As well, determining an appropriate value of Poisson's Ratio is difficult in this method, and in many cases it is simply assumed to be constant.

The approach followed in this study utilises the work of

Domaschuk and Valliappan (1974) in which the nonlinear behaviour of Winnipeg (Lake Agassiz) clays was characterised by non-constant bulk and shear moduli (K & G). Their study established a technique whereby these parameters were determined as functions of soil properties and stress level. The primary reason for choosing the deformation parameters K & G, is that each is associated with separate physical components of soil behaviour. The bulk modulus is associated with changes in mean normal stress, while the shear modulus is associated with changes in shear stress. Similarly, each can be evaluated independently by appropriate laboratory testing.

3.1 DEFORMATION PARAMETERS

In general, the state of stress at a point can be represented by three principal stresses and their respective direction cosines. For a cubical element, the magnitude and direction of these stresses can be represented by vectors acting on each face, as shown in Figure 1a. These principal stresses can be separated into mean normal components and deviatoric components as shown in Figures 1b and 1c, respectively. The mean normal stress (σ_m) and resultant deviatoric component (S_d) are given by:

$$\sigma_m = \frac{\sigma_1 + \sigma_2 + \sigma_3}{3} \tag{3.1}$$

$$S_d = \sqrt{S_1^2 + S_2^2 + S_3^2} \tag{3.2}$$

(a) General stress state

(b) Components equal to the mean normal stres:

$$\sigma_m = \frac{1}{3}(\sigma_1 + \sigma_2 + \sigma_3)$$

(c) Deviatoric components

$$S = \sigma - \sigma_m$$

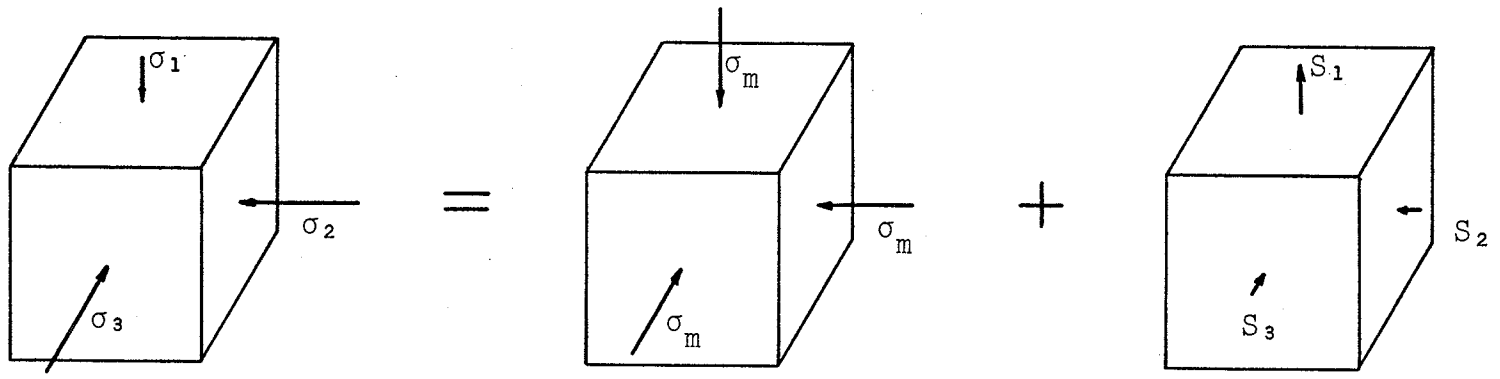

Mean Normal Component

σ_m

Linear strains producing volume changes

Resultant Deviatoric Component

$$S_d = \sqrt{S_1^2 + S_2^2 + S_3^2}$$

Shear strains producing distortion & dilatency

Figure 1: Typical State of Stress at Point

in which $S_1 = \sigma_1 - \sigma_m$, $S_2 = \sigma_2 - \sigma_m$, $S_3 = \sigma_3 - \sigma_m$

By the nature of its formulation, the mean normal stress (σ_m) is only associated with linear strains which result in volumetric changes. The resultant deviatoric component is associated with shearing strains which tend to produce distortion and dilatency effects. The mean normal strain (ε_m) and resultant deviatoric component (ε_d) are given by:

$$\varepsilon_m = \frac{\varepsilon_1 + \varepsilon_2 + \varepsilon_3}{3} \qquad (3.3)$$

$$\varepsilon_d = 2\sqrt{(\varepsilon_1 - \varepsilon_m)^2 + (\varepsilon_2 - \varepsilon_m)^2 + (\varepsilon_3 - \varepsilon_m)^2} \qquad (3.4)$$

The general constitutive relationship for a homogeneous, linear elastic material exhibiting small strains, can be expressed in terms of the bulk and shear moduli as follows:

$$\sigma_{ij} = K\,\varepsilon_{kk}\,\delta_{ij} + 2G\,(\varepsilon_{ij} - \tfrac{1}{3}\,\varepsilon_{kk}\,\delta_{ij}) \qquad (3.5)$$

where σ_{ij} & ε_{ij} = the stress and strain components respectively.

ε_{kk} = the cubical dilation.

δ_{ij} = the Kronecker delta.

Equation (3.5) can be resolved into a mean normal component, given by:

$$\sigma_m = 3K\varepsilon_m \qquad (3.6)$$

and a deviatoric component, given by:

$$S_d = G\varepsilon_d \tag{3.7}$$

3.1.1 Bulk Modulus

The bulk modulus is one of the constitutive parameters used in this study. It reflects only one physical component of behaviour and can be evaluated independently in the laboratory by drained isotropic triaxial compression tests.

The bulk modulus (K) which relates isotropic stress (σ_m) and volumetric strain (ε_v) was given in equation 3.6. Since the relationship is generally nonlinear, the bulk modulus may be defined as:

$$K = \lim_{\Delta\varepsilon_v \to 0} \frac{\Delta\sigma_m}{\Delta\varepsilon_v} = \frac{d\sigma_m}{d\varepsilon_v} \tag{3.8}$$

Several factors can affect the bulk modulus, particularly soil type, initial void ratio, the magnitude of isotropic stress, sample disturbance, etc. In the work of Domaschuk and Valliappan many of these were investigated. The results indicated the governing factors were soil type and isotropic stress level. The insitu void ratios fell in such a narrow range for each depth investigated, that they were not considered in the analysis. The expression used in the study was given by:

$$K_t = K_i \left(1 + n\varepsilon_{vn}^{n-1}\right) \tag{3.9}$$

where K_i = initial bulk modulus

ε_{vn} = normalized volumetric strain

The specific testing details and complete bulk modulus derivation can be found in Chapter IV of their report. A brief summary of that chapter can be found in Appendix A.

3.1.2 Shear Modulus

The shear modulus is the second constitutive parameter used in this study to describe soil behaviour. Like the bulk modulus, it reflects only one physical component of behaviour and can be evaluated independently in the laboratory. In this case the test required is a constant-mean-normal triaxial compression test.

The shear modulus (G), which relates the deviatoric stress (S_d) and the deviatoric strain (ε_d) was given in equation 3.7. Since the relationship is generally nonlinear, the shear modulus may be defined as:

$$G = \lim_{\Delta\varepsilon_d \to 0} \frac{\Delta S_d}{\Delta\varepsilon_d} = \frac{dS_d}{d\varepsilon_d} \qquad (3.10)$$

Domaschuk and Valliappan investigated several of the factors which affect the shear modulus, particularly the mean stress, void ratio, overconsolidation ratio, strength, sample disturbance, etc., in order to obtain a solution for the shear modulus of Winnipeg (Lake Agassiz) clays in a functional form. The expression used in their study was given by:

$$G = G_i\{1 - R_f(\frac{S_d}{10^{\alpha\{\frac{\sigma_m}{P'_c e_o}\}^{\beta}}})\}^2 \qquad (3.11)$$

in which G_i = initial shear modulus

R_f = failure ratio

S_d = resultant deviatoric stress

σ_m = effective-mean-normal stress

P'_c = preconsolidation pressure

e_o = initial void ratio

α & β = linear regression coefficients

The specific testing details and complete shear modulus derivation can be found in Chapter V of their report. A brief summary of that chapter can be found in Appendix B.

3.2 FINITE ELEMENT ANALYSES

The nonlinear stress-strain characteristics of Winnipeg (Lake Agassiz) clay, as per Domaschuk and Valliappan were incorporated in a nonlinear load-deformation finite element program. In this study, that program was used for the problem of predicting deformations associated with tunnelling in Winnipeg.

The most important consideration when using any finite element method program is that it does not yield exact solutions. At best, the solutions are very good approximations. The method relies on various 'approximate numerical methods' in its formulation as there are no closed-form solutions.

As well, there is always some doubt regarding the accuracy of the material properties used in the analysis. Consequently, the results are not exact, yet they are far better than any 'hand-method' or educated guess could ever offer.

Complete explanations of the finite element method can be found in several publications. Zienkiewicz (1971), Desai & Abel (1972), and Desai & Christian (1977) all explain the mathematical aspects of the method systematically, along with several applications of the method to various geotechnical problems. For completeness, a brief summary of the method follows.

In general, the finite element method consists of five separate steps. The first step is to discretize the global continuum into an equivalent system of smaller local continua called 'finite elements' as shown in Figure 2. The choice of orientation and size of elements is arbitrary. This allows the user to build a mesh which will account for nonhomogeneity (e.g. layered soils) with a minimum of difficulty. As well, by considering more elements in the analysis, the mathematical model is improved and more accurate results can be realised. However, this improvement is achieved at the expense of increased computing time.

The second step involves analysing each element in turn on the basis of its physical properties and constituitive relationships. Various methods of analysis, all derived from the principle of conservation of energy, are available for

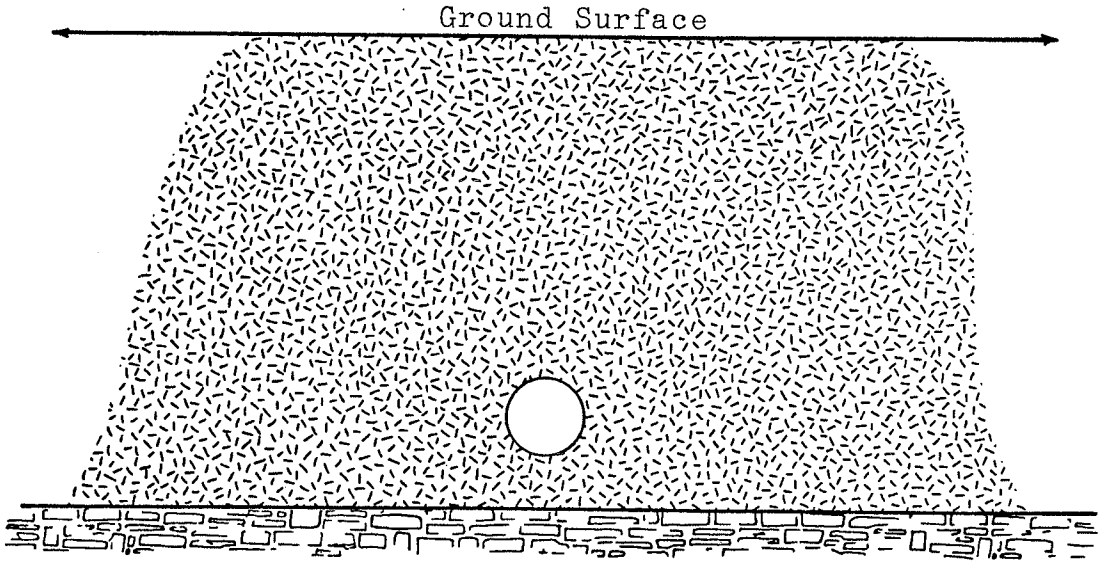

Figure 2a: Global continuum (plane strain) illustrating the tunnel and boundary conditions.

DEFINITIONS:

1. Centerline (axis of symmetry)
2. Nodal Line
3. Nodal Point
4. Finite Element
5. Loading
6. Flexible Boundary
7. Rigid Boundary

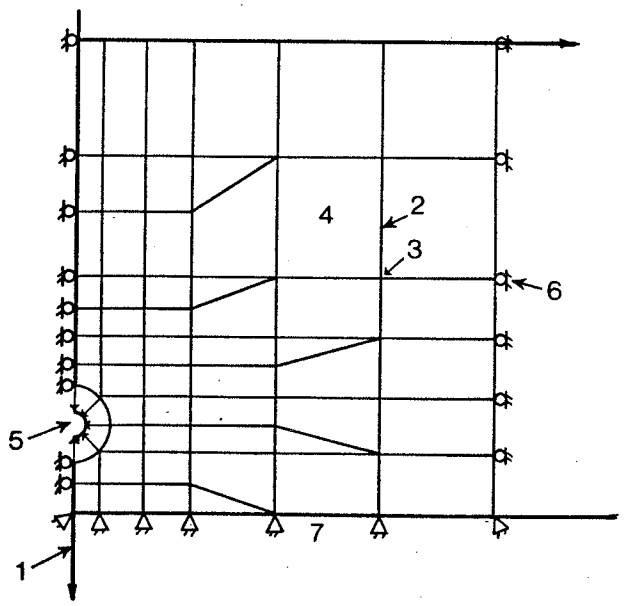

Figure 2b: Equivalent system illustrating finite elements.

this step. Commonly, minimum potential energy is used (Desai, 1977), that is, in any elastic body, the work done by the external static forces is stored optimally in the displaced shape as a minimum strain energy of distortion. The mathematical aspects of this step, often referred to as the Displacement Method, are presented in Appendix C.

The third step in the finite element method is referred to as the Direct Stiffness Method. This step assembles the local element stiffness matrices into a global stiffness matrix using the principle of superposition. As each element has been analysed locally, the stiffness of any given node is based only on that element. In the global system, any given node may interconnect any number of elements. The total stiffness of the node is the summation of all of these elements. This process satisfies the compatibility of displacements at the nodal points relative to the global continuum. It does not satisfy the displacement compatibility along the element's edges.

The final two steps involve combining the known boundary conditions and external loadings with the global stiffness matrix of step three, thus satisfying the equilibrium of the system. The equations are then solved, yielding first the unknown displacements and second the element strains and stresses.

For the particular study dealt with in this project, a plane strain, nonlinear finite element program was used for

the analysis. Many three-dimensional problems, such as tunnelling, can be modelled in two dimensions. The simplification arises from the fact (or assumption) that the displacements of the system are developed only in one plane. For the problem of tunnelling, it is generally assumed (Ghaboussi et al, 1978) the tunnel is excavated instantaneously such that the displacements are only radial, ignoring any in the axial direction. The result is a two-dimensional problem that need only consider a strip of unit thickness as shown in Figure 3.

3.2.1 Nonlinear Analyses

The basic concept of the finite element method is independent of whether linear or nonlinear analysis are performed. However, certain factors must be considered when doing nonlinear analyses. The first step is to choose the type of nonlinear behaviour associated with the problem.

In general, nonlinear behaviour can be divided into three categories:

1. Material nonlinearity, which arises from nonlinearities in the constitutive equations.
2. Geometric nonlinearity, which arises from large deformations and geometric changes in the structure and elements.
3. Combined geometric and material nonlinearity.

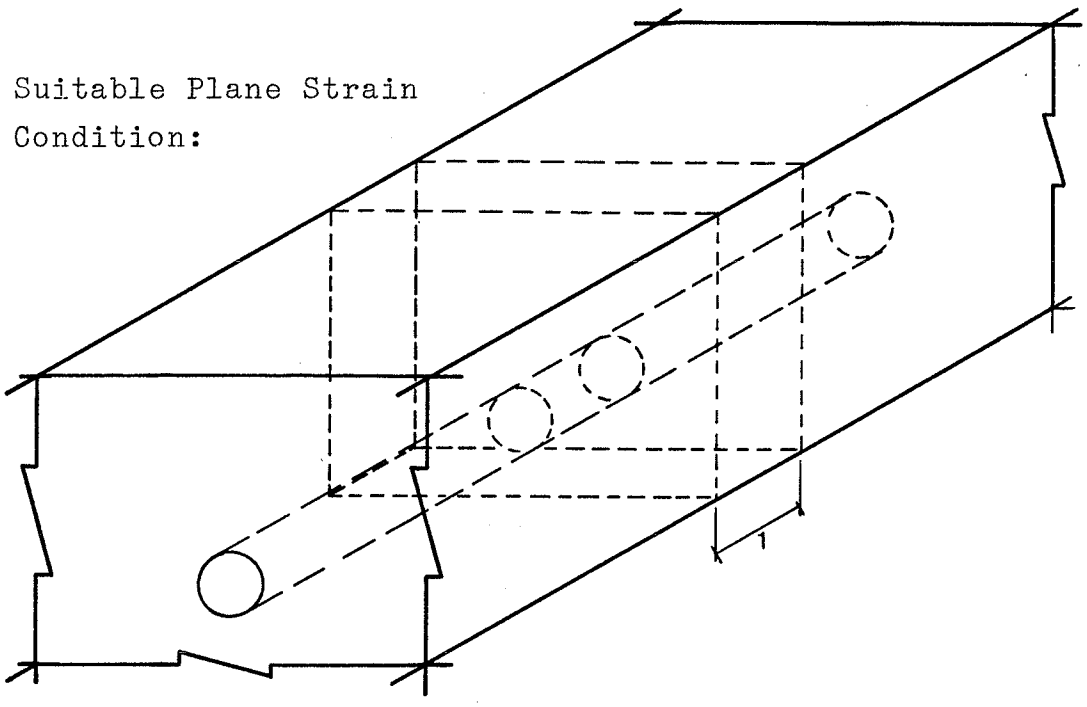

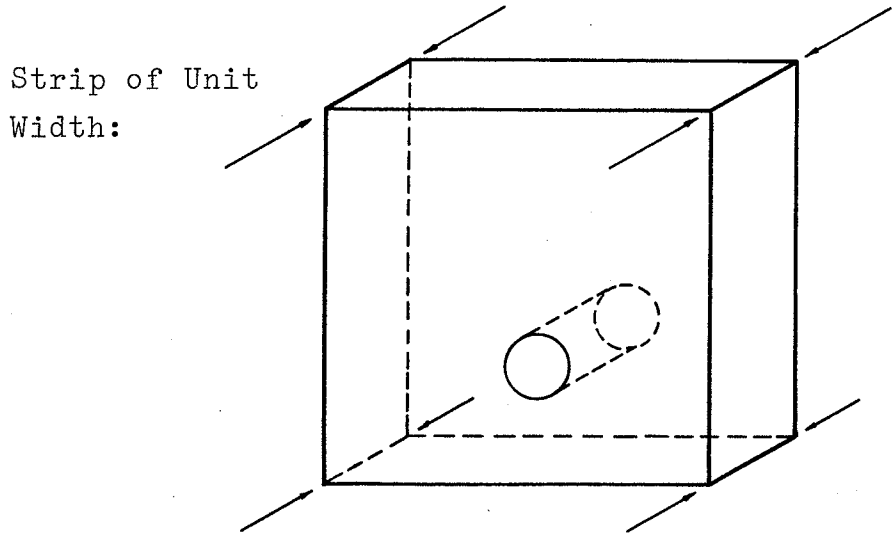

Figure 3: The three dimensional problem of tunnelling can be modelled in two dimensions by taking advantage of the symmetry of the system.

In this study, the effect of geometric nonlinearity was expected to be insignificant as the displacements under the normal range of loads are small relative to the dimensions of the continuum. Consequently, this study has been concerned only with material nonlinearity.

As described in Chapter II, in order to simulate any nonlinear behaviour it is necessary to adjust one or more of the deformation parameters in accordance with internal stress changes. This implies that they must reflect changing stress conditions resulting from load application and/or removal. In this study, the adjustment was made to the stress-strain matrix [C], and is known as the variable or tangent stiffness method. Clearly to make these adjustments an iterative approach was mandatory.

The simplest and most common iterative solutions involve an incremental or stepwise procedure. The basis of this technique is to subdivide the load into a number of small increments, and apply them one at a time. At the beginning of each new load increment approximate moduli values are selected for each element on the basis of the existing stresses and strains in that element. The load increment is then applied and the resulting stress, strain, and displacement changes are calculated and added to the previous values. These new values are used to establish new moduli values.

Another common technique, referred to as the midpoint Runge-Kutta procedure, determines a new [C] matrix for the

stresses and strains associated with applying one-half of the load increment. This stiffness matrix is then used for computing the stresses and strains for the required full increment. As with the full increment method, the change in stress and strain are added to the previous values, and the procedure is repeated until the entire load has been applied.

Essentially, these techniques approximate nonlinear behaviour as a series of linear steps as shown in Figure 4. Obviously the more steps taken in reaching the total load, the better the accuracy. Unfortunately, this accuracy is achieved at the cost of additional computer time as new stress-strain matrices must be determined for all elements in each load increment. The program used in this study incorporated both nonlinear techniques.

3.3 THE FINITE ELEMENT PROGRAM

The finite element program investigated in this study was originally developed by Domaschuk and Valliappan in 1974 to analyse the stresses and displacements of various nonlinear axisymmetric problems in geotechnical engineering.

The program had two main features which made it particularly useful to this study: first, the constitutive portion of the program made use of either Young's Modulus (E) & Poisson's Ratio (ν), or the Bulk Modulus (K) & Shear Modulus (G) as the deformation parameters; and second, the program had been designed specifically for a nonlinear analysis of the Winnipeg (Lake Agassiz) clays.

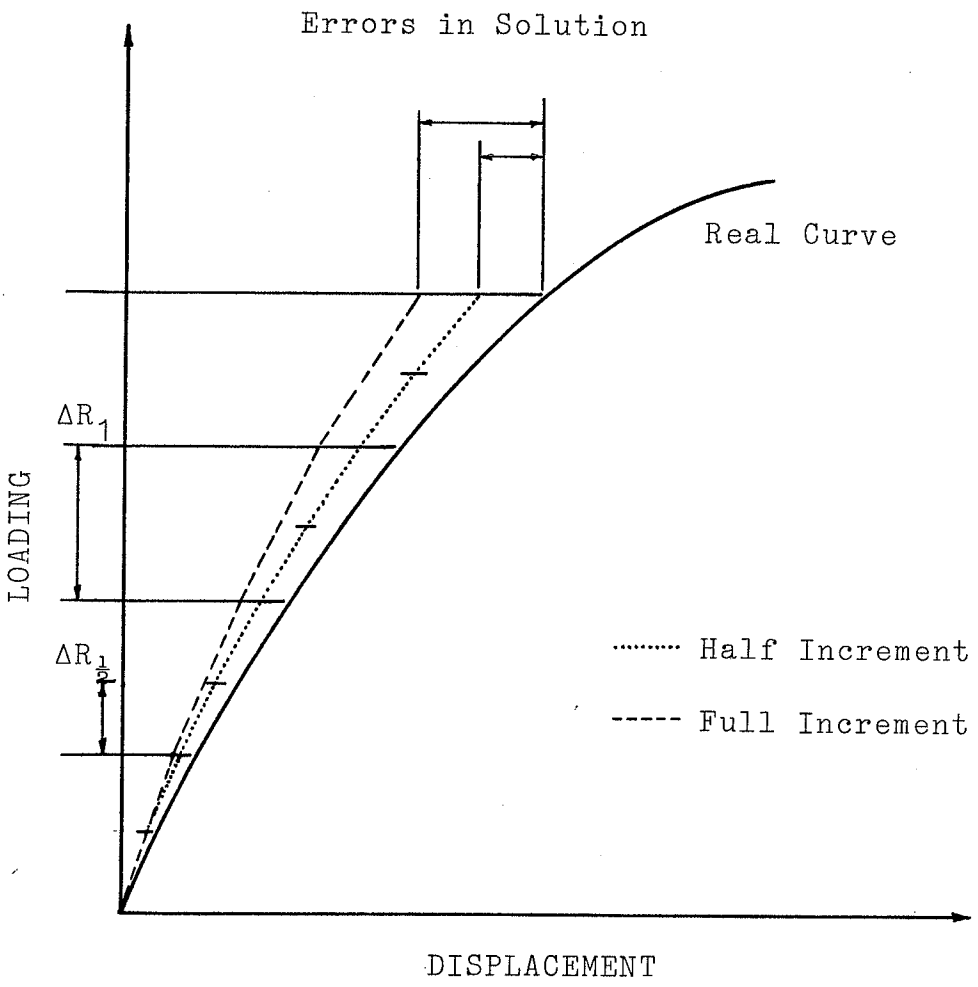

Figure 4: Full and Half Incremental Methods of non-linear analysis.

The basic formulation of the program (i.e. the element and global stiffness matrices, the equation solver, and the stress solution) follows the one developed at the University of California by Wilson (1967). The basis for the incremental method of nonlinear analysis follows a program developed by Desai (1968). Since its formulation, the program was only used on one or more occasions. Recently, Yong (1983) studied the contribution of the bulk and shear moduli to displacements using the program. As a result the program was better detailed and also updated to handle metric units. The program has since been modified to suit the requirements of the particular tunnelling problem being considered.

In an attempt to model the tunnelling operation it was decided to change the program's axisymmetric formulation to that of a plane strain problem. By simply replacing the components of the third row and column of the stress-strain matrix with zeros, the program automatically recognized the plane strain condition.

A second modification to the program was required to keep the shear modulus (G) from going to zero in the iterative solutions. The need for doing this arises from the fact that some of the elements go into a plastic stress state at large boundary loads, before a general state of failure has occurred. The method chosen involved limiting the change and/or magnitude of the shear modulus to some minimum value. The program changes necessary for this modification only

affected the subroutine which calculated the shear modulus.

The first step was to limit the change of decreasing shear moduli between successive iterations to some arbitrary value. The number chosen was given by:

$$\Delta_{max} = \frac{1}{\#\ increments}$$

If the calculated change exceeded this value, a revised shear modulus (G_{new}) was given by:

$$G_{new} = (1 - \Delta_{max}) * G_{old}$$

This implied if 5 increments were specified, the maximum change in any given increment would be 20%.

The second step was to establish a lower bound on the shear modulus. This was chosen to be 1350kPa.

CHAPTER IV

4.0 MODELLING THE TUNNEL PROBLEM

4.1 TUNNEL DETAILS

In July 1978, Hardy Associates (1978) Ltd. and R. V. Anderson Associates Ltd. began a Tunnel Instrumentation Project for the City of Winnipeg, Waterworks, Waste and Disposal Division; the objective being to enhance the design and minimize the cost of future tunnel construction in the Winnipeg area.

Located near the North End Water Pollution Control Plant in Northwest Winnipeg, the tunnel strikes east to west at a centerline depth of 12.7 m, with a 2.0 m outside diameter. The tunnel was hand-mined without a shield at a rate of approximately 3.0 m per day. Primary lining was not required. The interior formwork consisted of steel ribs and timber planks, which were also removed at a rate of 3.0 m per day following a curing period of 3 days. Liner concrete was placed to within approximately 1.0 m of the tunnel face each day.

The tunnel was monitored at the Northwest Interceptor, some 50 m west of the northwest corner of the treatment plant site. The soil and liner instrumentation used at the site included piezometers, settlement plates, a slope indicator, earth pressure cells and embedment strain gauges. The

instrumentation layout is shown both in plan and section in Figure 5. Details of the instrumentation can be found in Chapter 3.0 of Hardy's report (1981).

4.2 SOIL INFORMATION

4.2.1 Sources of Information

The geotechnical information used in this study was correlated from two sources; the detailed site investigation conducted by Hardy Associates (1978) Ltd. and a report on the nonlinear behaviour of Lake Agassiz clays by Domaschuk and Valliappan (1974).

4.2.2 Soil Profile and Index Properties

Hardy's investigation, which was done at the location of the riser pipe shown in Figure 5, included the usual routine sampling along with several vane shear and pressuremeter tests. The results of the testing program, along with the test borehole log, are shown in Figure 6.

Soil stratigraphy at the instrumentation site is typical of the Winnipeg area, being comprised of a thin cover of top soil over varved, lacustrine clays. The surficial clay deposits are brown, becoming mottled from about the 2 m depth and grey from about the 7 m depth. The transition in color is gradual. A 1 m layer of tan silt exists within the upper 3 m of the profile. The clays are highly plastic (CH) with

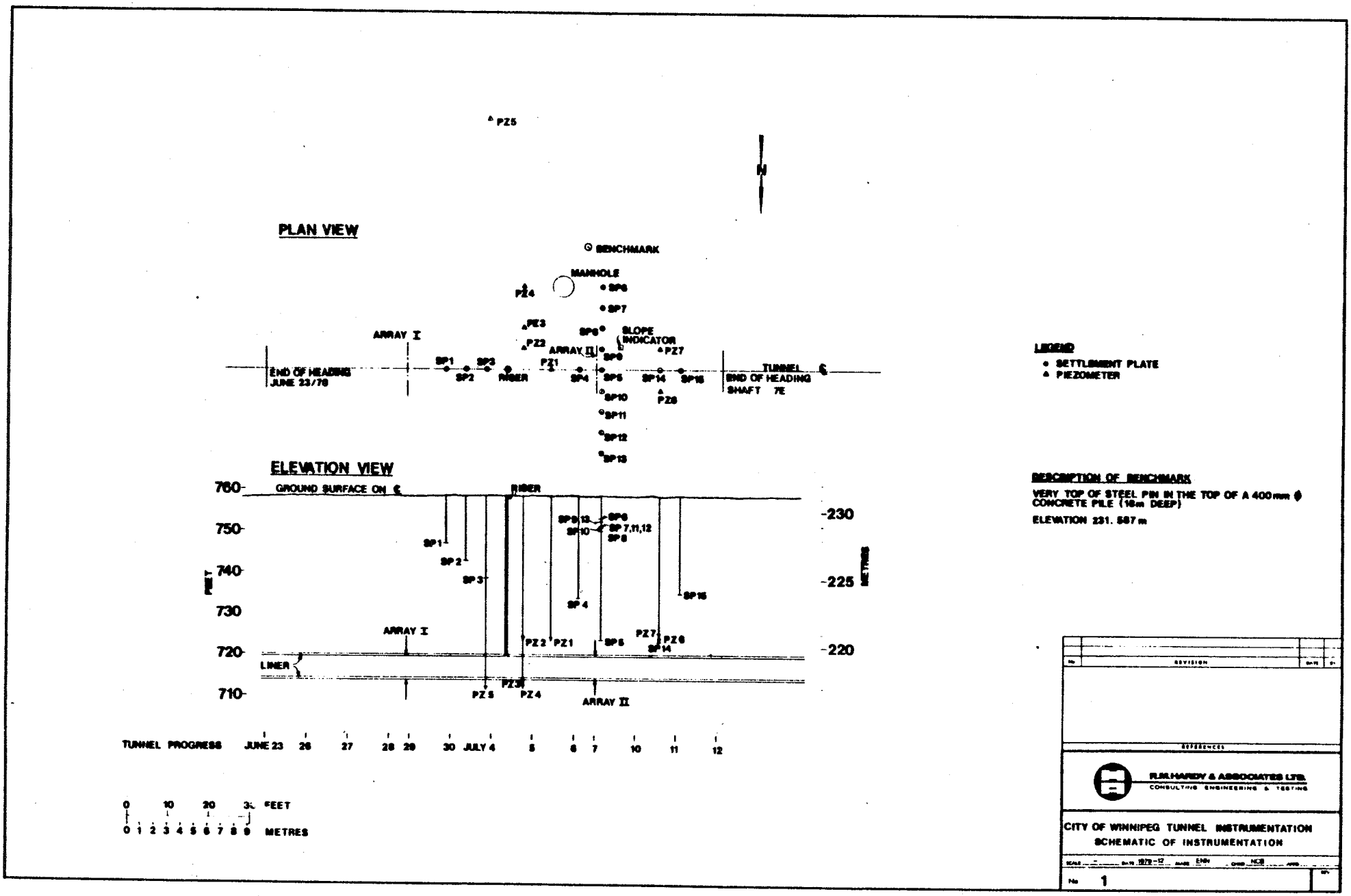

Figure 5: Tunnel Instrumentation Layout
After Hardy et al (1981)

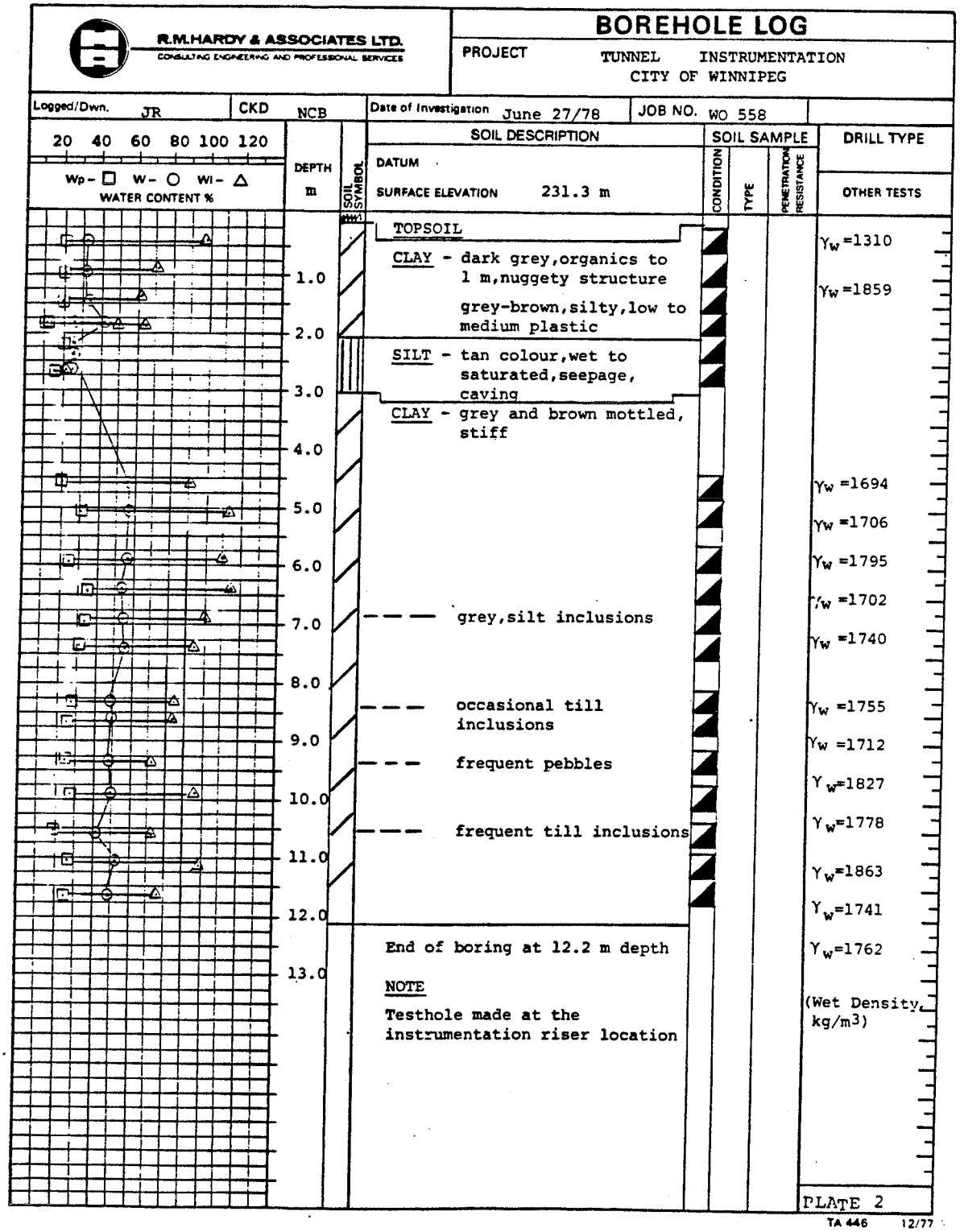

Figure 6: Original Borehole Log, After Hardy et al (1981)

plasticity indicies ranging from 40 to 77, and tend to decrease slightly with depth.

The moisture content profile is relatively uniform with some evidence of drying or dessication within the surficial 3 to 4 m depth. Bulk densities ranged from approximately 16.3 to 18.3 kN/m^3. Undrained shear strengths varied from approximately 50 to 125 kPa based on field vane shear tests and 25 to 60 kPa based on unconfined compression tests.

4.2.3 Properties Chosen for Finite Element Modelling

The borehole log contained in Hardy's report extended only to 12.2 m, while the dimensions of the finite element model required a depth of approximately 17 m. The remainder of the basic geotechnical data (moisture contents, specific gravities, plasticity indicies) were obtained from Domaschuk and Valliappan (1974) in the belief their study was representative of the Winnipeg area (Baracos, 1961). The extended borehole and associated data is shown in Figure 7.

Where possible, the basic geotechnical data used in the program was compared with published values (Graham et al, 1982) to assure reasonable magnitudes were being considered. In the program output, the calculated insitu bulk and shear moduli were also observed and are shown in Figures 8 and 9. The calculated bulk modulus shows excellent correspondence with Graham's work, while the shear modulus shows only satisfactory correspondence.

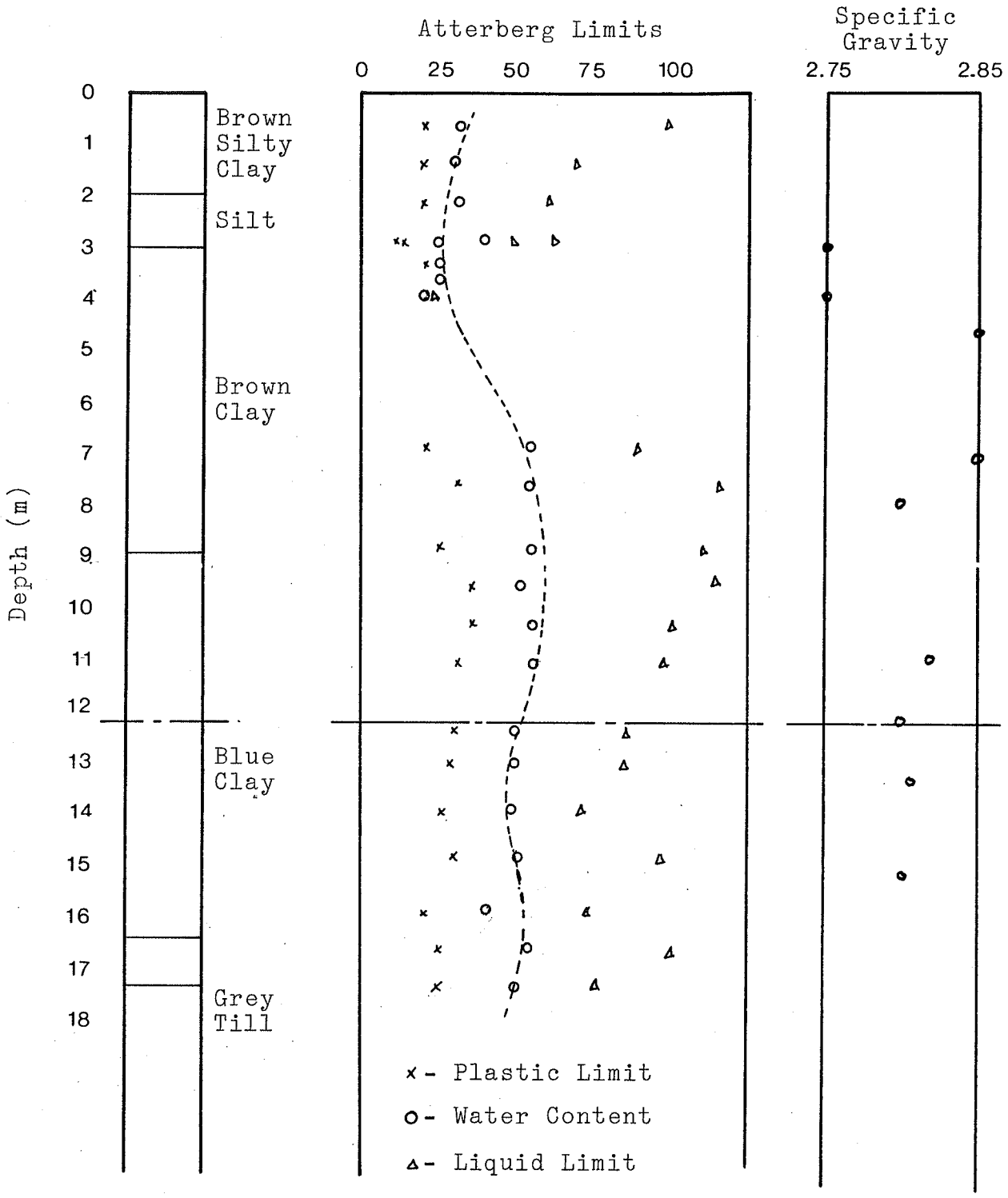

Figure 7: Extended borehole and associated data. After Hardy et al (1981) and Domaschuk and Valliappan (1974).

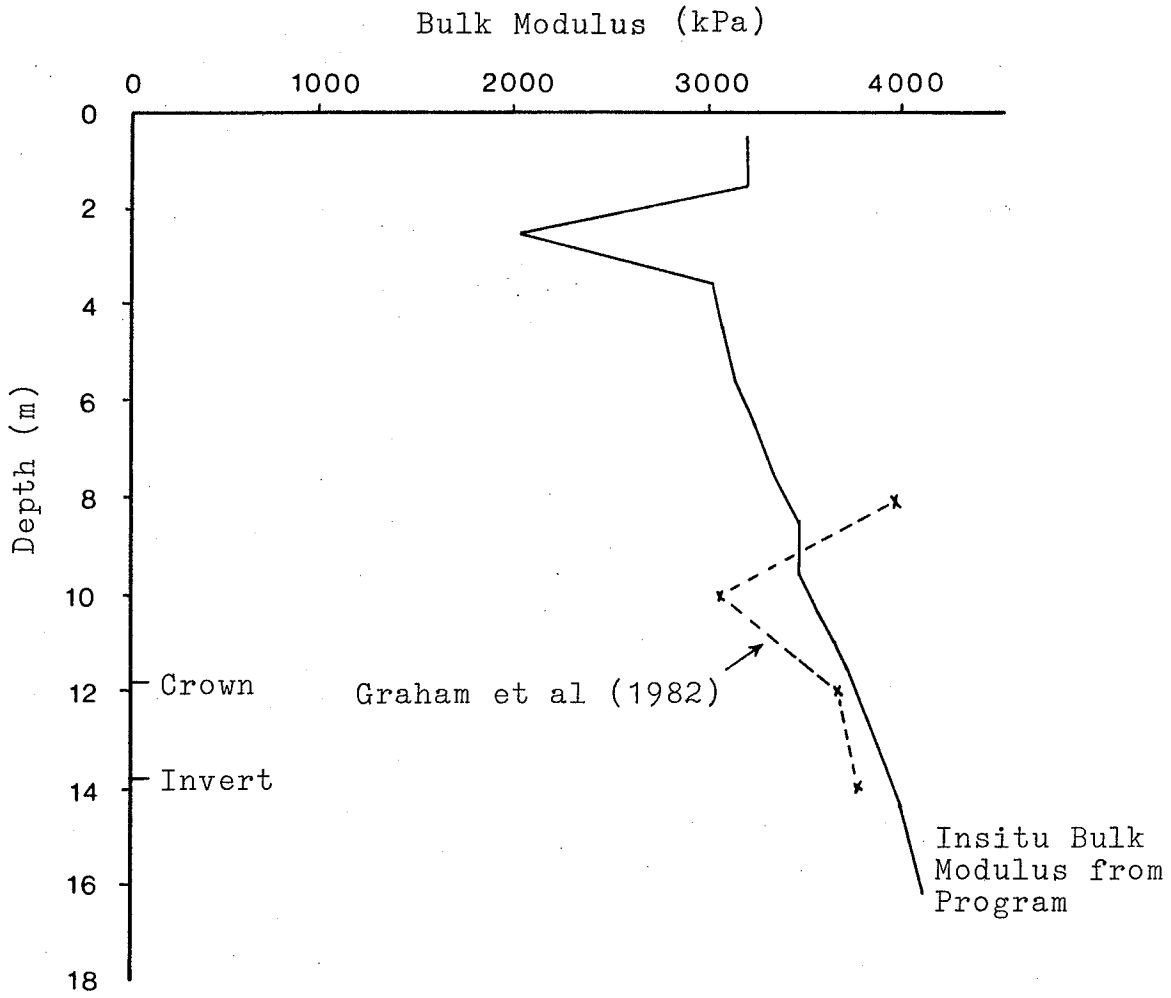

Figure 8: Insitu Bulk Modulus from Program vs. Graham et al (1982)

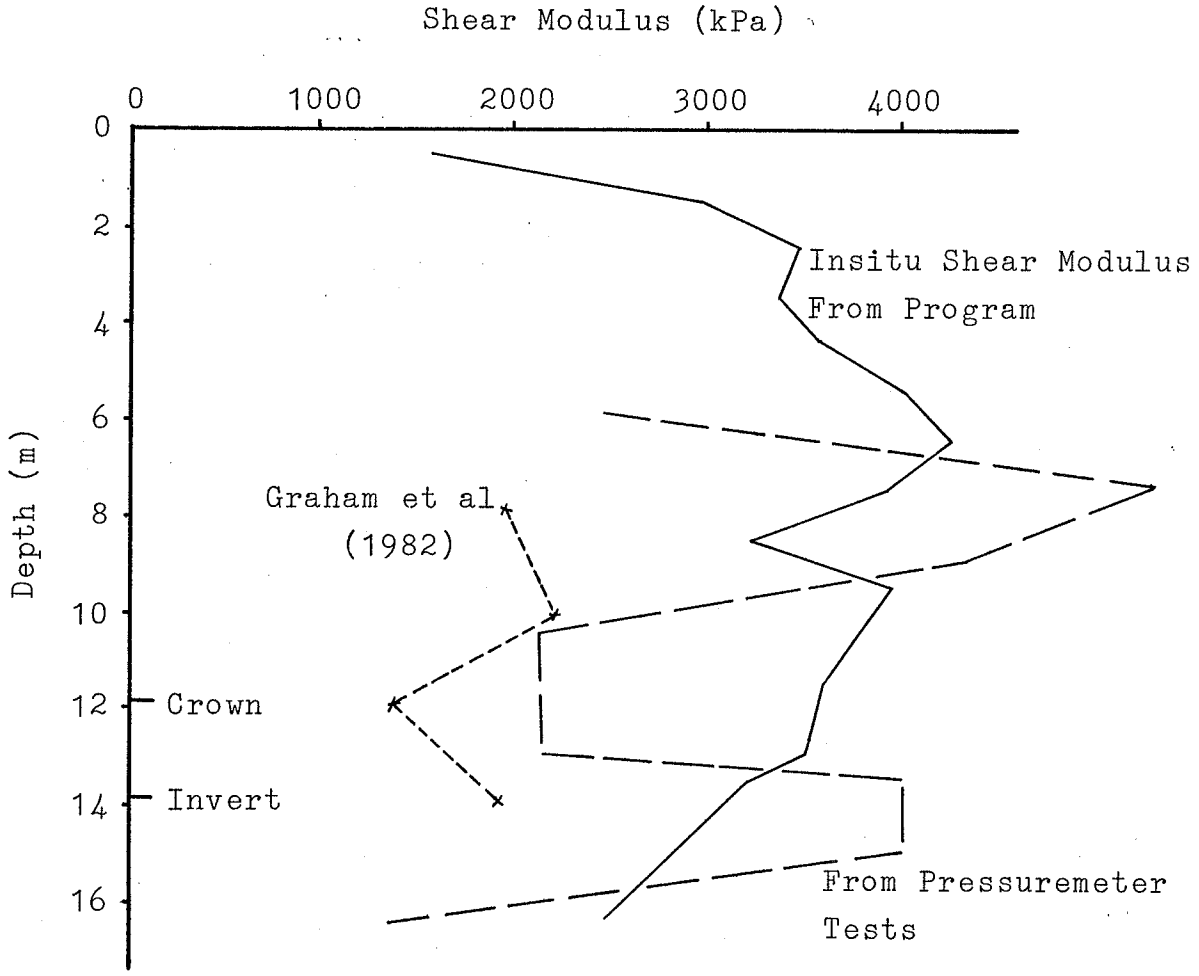

Figure 9: Insitu Shear Modulus from Finite Element Analyses vs Graham et al (1982) and Pressuremeter Results

The nonlinear behaviour of the Lake Agassiz clays used in this study have been described by the failure criterion developed by Domaschuk and Valliappan (1974). The failure criterion, which is in terms of resultant deviatoric stress at failure and constant-mean-normal stress has the advantage of incorporating the effect of the intermediate principal stress. As well, it does not require the orientation of the failure plane for comparing the prevailing state of stress to the failure stress at any point within the mass. A complete description of the failure criterion formulation can be found in Appendix B. For the purpose of clarity, it is expressed here as follows:

$$S_{df} = 10^{\alpha\{\frac{\sigma_m}{P'_c e_o}\}^{\beta}} \qquad (4.1)$$

in which S_{df} = resultant deviatoric stress at failure

P'_c = preconsolidation pressure

σ_m = effective-mean-normal stress

e_o = initial void ratio

α & β = linear regression coefficients in log-log plotting, referred to as failure criterion parameters

Clearly these parameters were not contained in Hardy's site investigation, and consequently they had to be interpreted solely from Domaschuk and Valliappan's report on the basis of physical descriptions of the materials.

The coefficient of horizontal earth pressure (Ko) was intentionally chosen equal to 1.0 to facilitate calculating the boundary loads on each element in the tunnel. The need for this assumption arises because the program can not distinguish what portion of the applied load is vertical and which is horizontal on the elements with sloped faces. It should be noted that this assumption is common in other finite element studies such as Hoyaux and Ladanyi (1969) and Hardy et al (1981).

4.3 FINITE ELEMENT MODEL

The finite element model used in this study is shown in Figure 10. It contained 165 elements, 186 nodes, and was separated into 4 different soil types within the continuum. The general orientation and dimensions of the model are similar to those used by Hardy et al (1981) thus allowing correlation between the two studies.

As described previously, the borehole log shown in Figure 7 is typical of the Winnipeg area, and specifically the tunnel site, and implies there is symmetry about any vertical line in the continuum. This symmetry allowed the modelling of only one-half of the continuum (in the horizontal direction) using the centerline of the tunnel as the axis of symmetry and one vertical boundary. The second vertical boundary was placed 7 tunnel diameters away, where it was assumed boundary influences would be at a minimum. Both

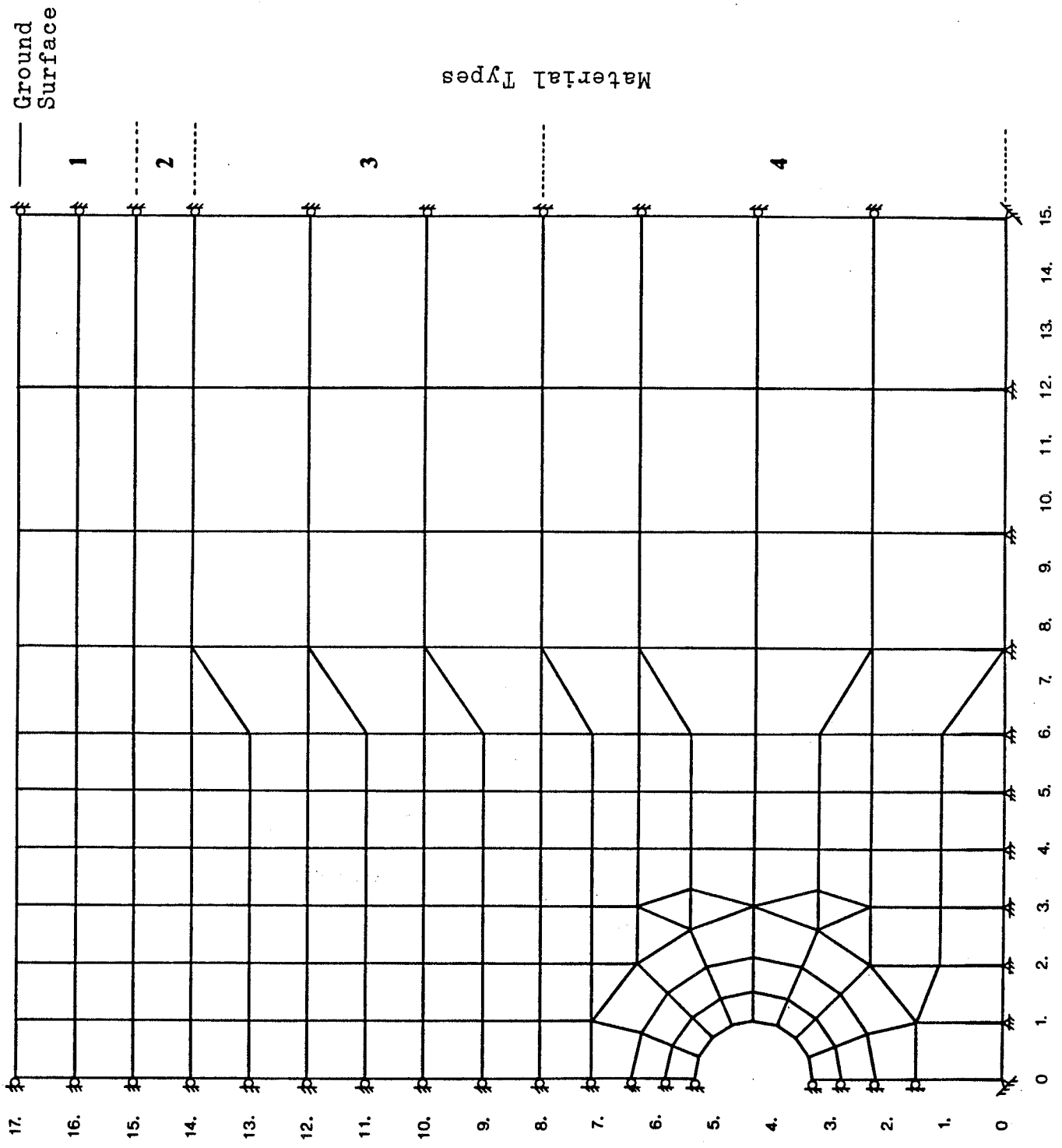

Figure 10: Finite Element Mesh

of these boundaries (with the exception of the tunnel opening) were considered restrained in the horizontal direction, allowing only vertical displacements.

The upper horizontal boundary (ground surface), located 11.7 m above the tunnel crown, was considered to be unrestrained in all directions. The lower boundary was located 3.3 m below the tunnel invert and was considered to be restrained in all directions. Finally, the nodes making up the tunnel opening were considered to be unrestrained in all directions.

4.3.1 Boundary Load Conditions and Deformation Analyses

In order to model the physical operation of tunnelling with a finite element program the user must be aware of the program's formulation, particularly the technique used to build the load vector. Although several programs consider gravity forces as loads, this particular one does not. Gravity forces are only used to calculate insitu stresses and subsequent bulk and shear moduli values for each element; they are not considered as loads. When the analysis is performed, the program considers the continuum weightless, and calculates only the stress change associated with that load application, either compressive or tensile. These changes are then added to the previous stress values yielding a new stress state from which revised bulk and shear moduli values can be determined. This procedure is continued until all

iterations have been completed.

The implication is that to model the tunnelling operation the user must apply the negative of the insitu stress, as calculated at the center of the face of each element around the tunnel opening, divided by the number of increments. In this study the insitu stresses vary from a minimum of -203.275 kPa at the crown to a maximum of -236.145 kPa at the invert. This is simply the result of the change in depth from the top to the bottom of the tunnel opening.

Four load cases have been considered in this study. The first one investigated the insitu to zero stress in one step, i.e. - a linear analysis. The second, third and fourth cases investigated the insitu to zero stress in two, five and ten steps respectively.

As described previously, the program calculated the insitu bulk and shear moduli on the basis of input soil parameters, namely moisture contents, plastic indicies, unit weights, etc. The loading magnitude has absolutely no effect on these insitu values, and consequently the starting point for each analysis was always the same.

CHAPTER V

5.0 RESULTS AND ANALYSIS OF RESULTS

The results of the deformation analyses have been separated into three parts; first, an investigation of the linear and nonlinear analyses, second, a comparison of the finite element results with measured field values, and third, a discussion of the results.

5.1 LINEAR VS NONLINEAR ANALYSES

Figure 11 illustrates typical displacement vectors along three radial directions extending from the tunnel center. The results clearly indicate that the majority of deformation is directed toward the tunnel center.

Figures 12 and 13 illustrate the magnitude of deformation along the vertical and horizontal radials respectively for each load case. The vertical radial, located directly above the tunnel crown shows deformations ranging from 6.5 mm for the linear case to 12.2 mm for the 10 increment nonlinear case. The horizontal radial, which extends from the tunnel center, shows deformations ranging from 11.7 mm for the linear case to 16.1 mm for the 10 increment nonlinear case. The results indicate a zone of influence exists around the tunnel opening which ranges from 2 to 4 tunnel radii along the vertical radial and up to 6 radii along the horizontal.

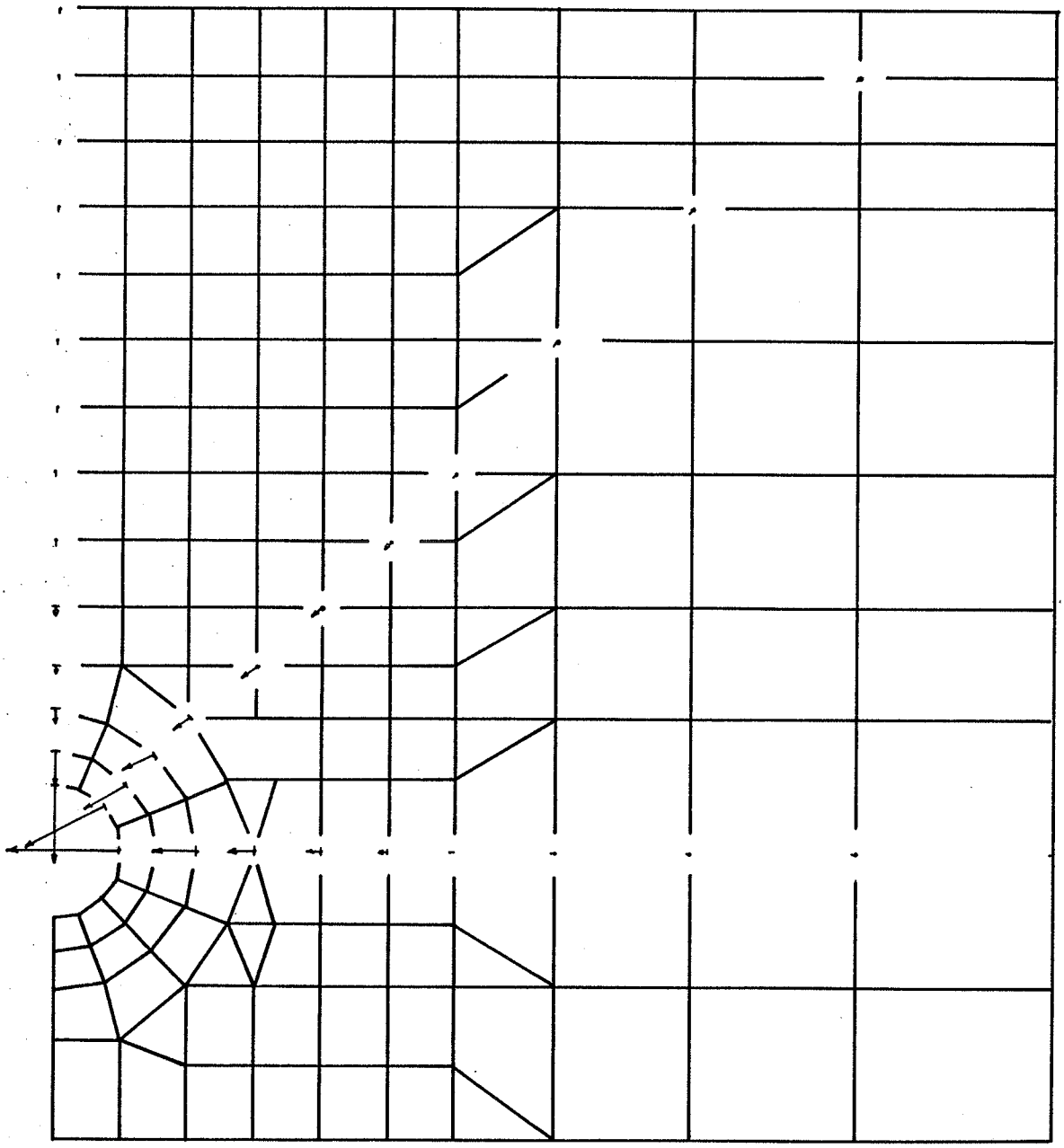

Figure 11: Typical Displacement Vectors from Finite Element Analyses

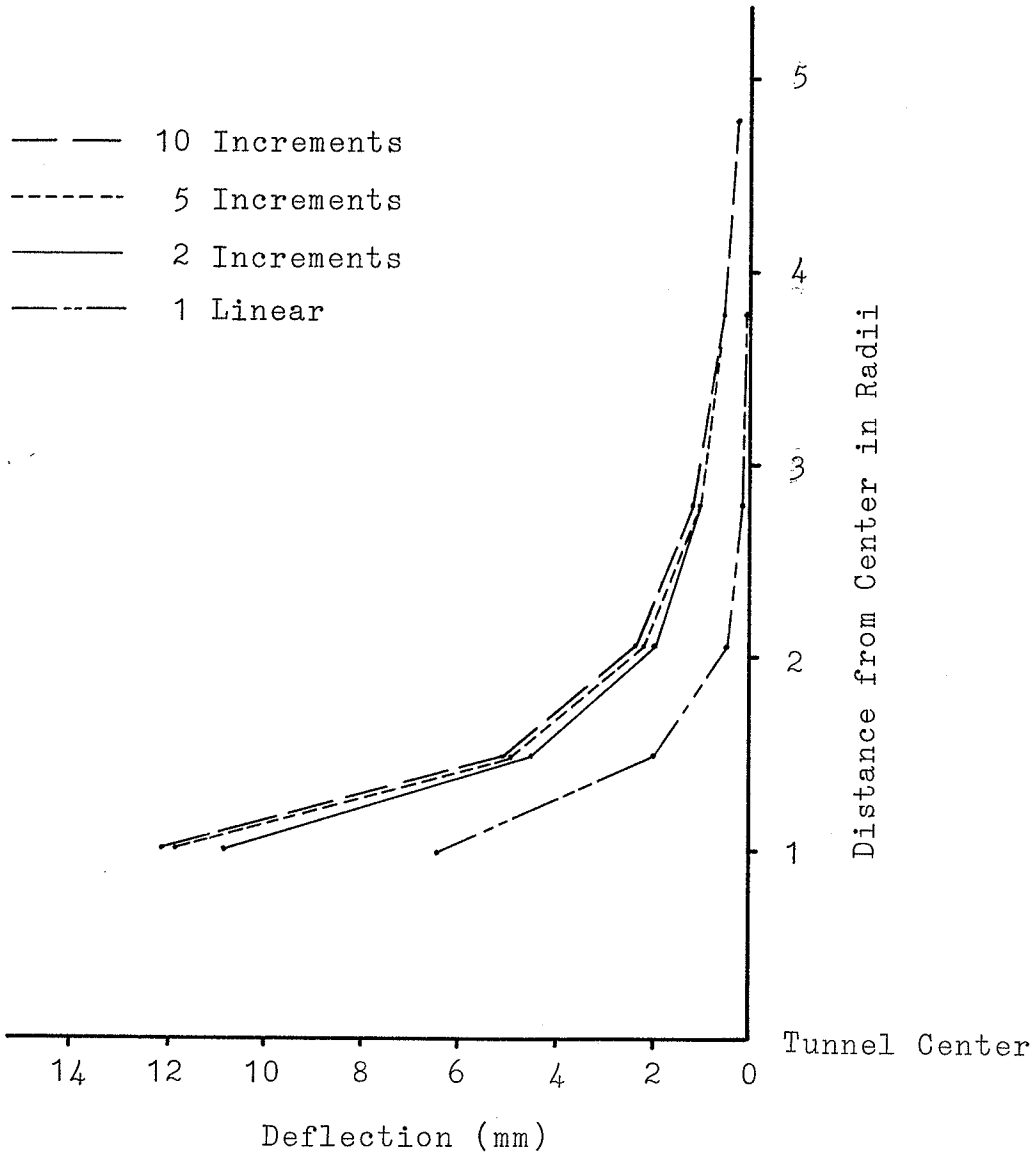

Figure 12: Magnitude of Deformation Along the Vertical Radial

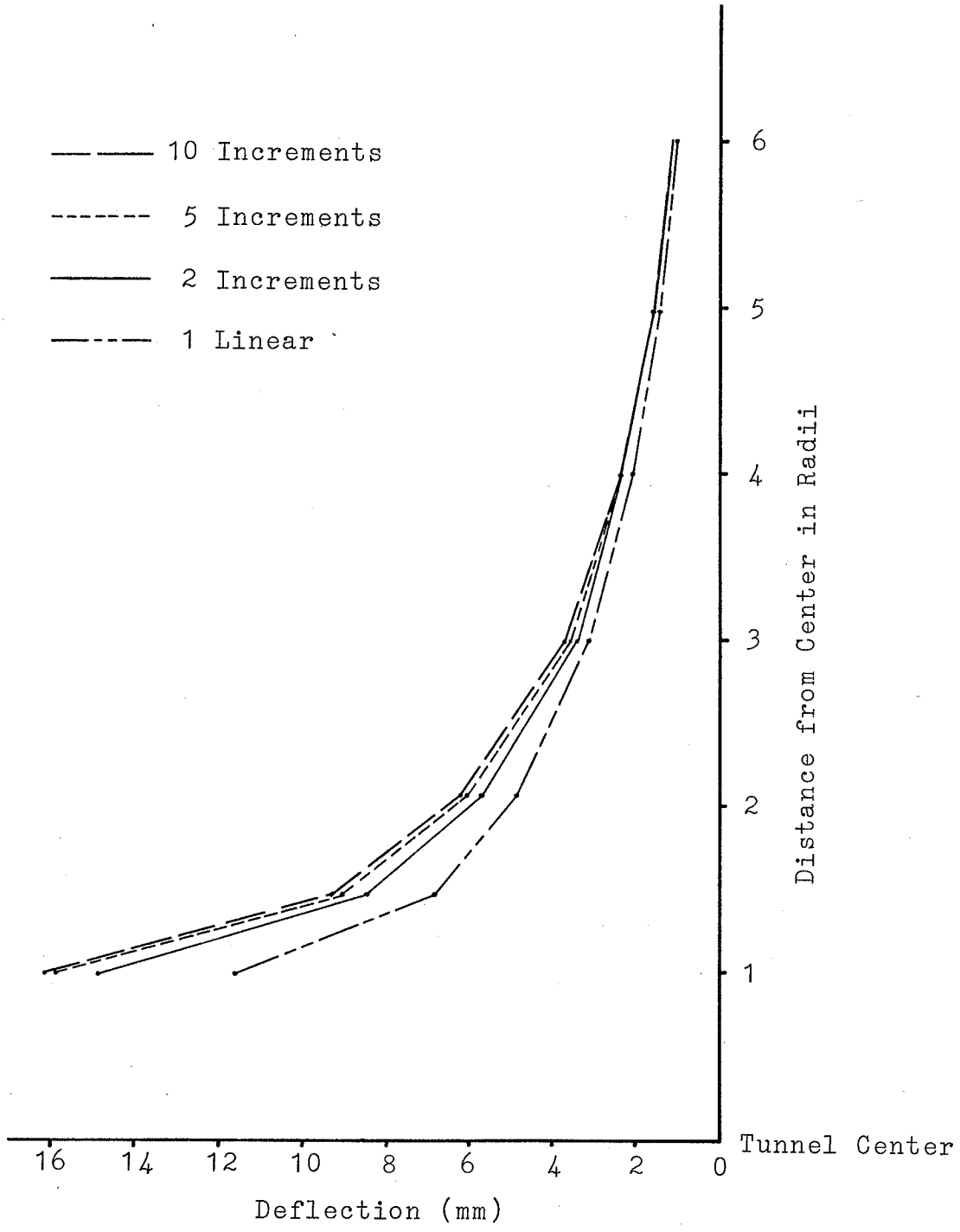

Figure 13: Magnitude of Deformation Along the Horizontal Radial

In Figure 14, the deformations at the tunnel wall were plotted against the number of increments into which the total boundary load associated with excavation, was divided. The use of a single increment was in effect a linear analysis as the deformation analysis was done using only a single average value of the bulk and shear moduli in each element. Dividing the total boundary load into 2 or more increments rendered the analysis nonlinear in that the deformation parameter's magnitude changed with each load increment in each element. From Figure 14 it is seen that the nonlinear analyses resulted in a substantial increase in the computed deformations, with the largest increase being associated with the 2 increment analysis. The increase from five to ten increments was insignificant.

As described previously, the starting point (i.e. - the insitu values) for both the bulk and shear moduli was the same for all load cases. However, the magnitude and rate of change of these parameters during the iterative solutions was dependent on the number of increments into which the total boundary load was divided. The dependence of the two deformation parameters on the prevailing state of stress in the soil was examined by plotting the deformation parameters for each iterative solution.

The bulk modulus values associated with the iterative solutions decreased with load removal, as anticipated. However, the magnitude of change was insignificant and could not

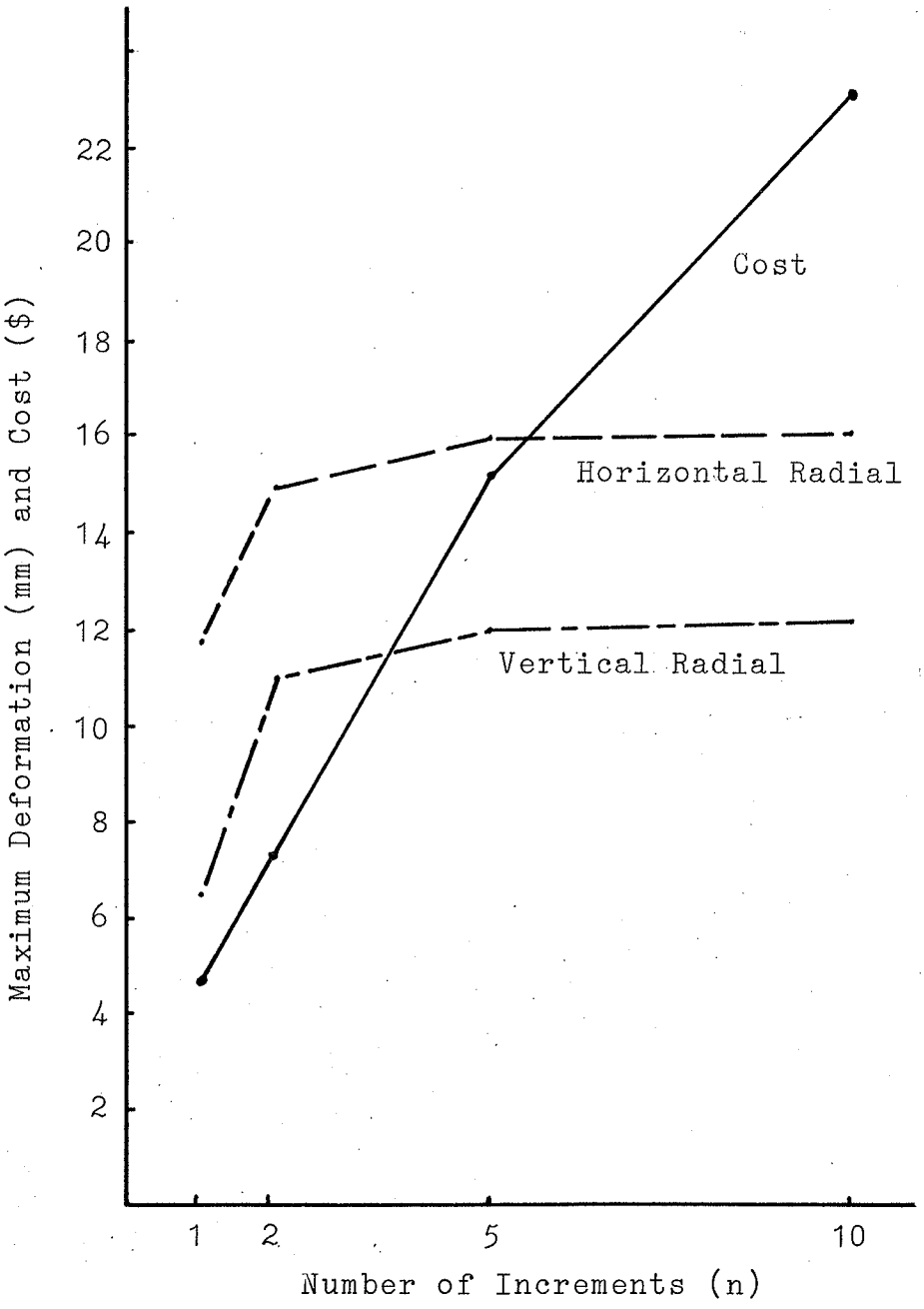

Figure 14: Maximum Deformation and Cost vs Number of Iterations for the Vertical and Horizontal Radials

be plotted separately from the insitu line shown previously in Figure 8. Clearly the bulk modulus was not a significantly contributing factor to the nonlinearity of the analysis. The results indicate that the bulk modulus could be considered a constant for any given element throughout the analyses.

The shear modulus of each element along the vertical radial is shown for the insitu case and for each loading case in Figure 15. For any given element (represented by a constant depth) the shear modulus decreased at a decreasing rate as the number of load increments was increased. It is apparent that the use of a single "insitu" modulus would yield smaller calculated deformations than the use of a stress-dependent modulus which decreases in magnitude as the state of stress in the soil tends toward failure.

Increasing the number of increments into which the total load is divided may be thought of as a refinement of the nonlinear analysis. For the tunnel case analysed in this study, the use of more than 5 increments did not significantly change the calculated deformations, and so from an "accuracy" point of view, 5 increments were sufficient.

The computer costs associated with the various load cases used are shown in Figure 14. It is seen that in an approximate way there was a direct relationship between computer costs and the number of load increments used. Thus from a standpoint of costs, the number of increments should be kept to a minimum.

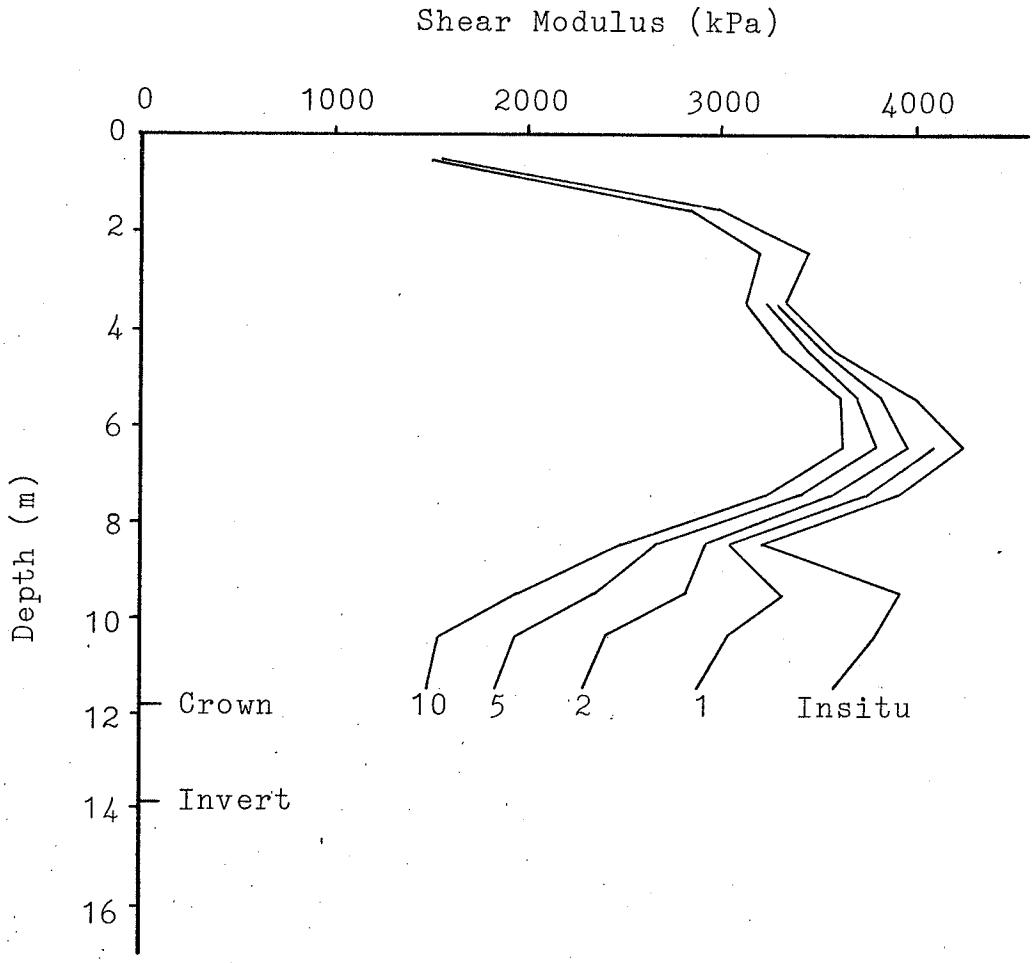

Figure 15: Variation of Shear Modulus Values with the Number of Increments

5.2 COMPUTED DEFORMATIONS VERSUS OBSERVED DEFORMATIONS

A comparison of measured field deformations along the vertical radial with those computed using the nonlinear analysis with 10 increments is shown in Figure 16. It is seen that the comparison is good at the tunnel wall where the observed deformation was 14 mm and the computed was approximately 13 mm. Thus from the standpoint of a Class A prediction of tunnel deformations, the mathematical model proved to be very accurate. However the agreement between the predicted and observed at points away from the tunnel wall was very poor. According to the mathematical model, significant deformations were confined to a distance of only one tunnel radius beyond the tunnel wall, whereas the observed deformations extended beyond 6 tunnel radii. As well, the deformation patterns were quite different throughout the continuum. The observed deformations varied almost linearly with depth whereas the predicted values approached zero asymptotically.

5.3 DISCUSSION OF RESULTS

The reasons for the variation between observed and predicted values are associated with either the input data or the mathematical model used.

Insofar as input data is concerned, the insitu soil properties used were those of another site but because of the similarities of the soil conditions at the two sites, it is

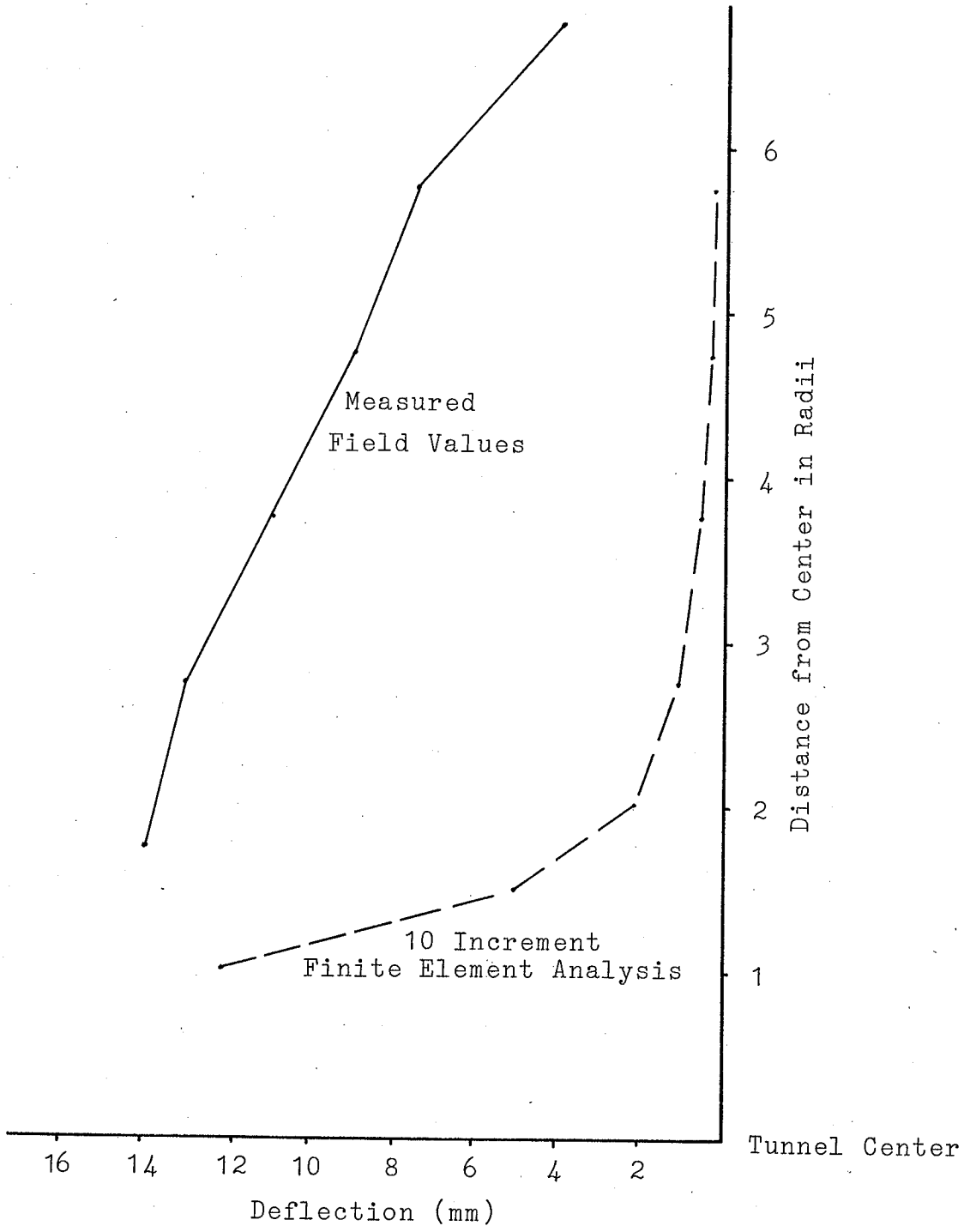

Figure 16: Comparison of the 10 Increment Finite Element Analysis and Measured Field Values Along the Vertical Radial

unlikely that this was a significant contributing factor. However the solutions for the bulk and shear moduli are functions of stress and were determined by laboratory compression tests whereas the tunnel problem, was one of unloading. It was assumed in the deformation analysis that the solutions for the deformation parameters were not stress-path dependent. This could account for some discrepancy between observed and predicted values, but was unlikely the major factor.

As mentioned previously, the greatest discrepancy between observed and predicted values was in the pattern of deformation versus radial distance from the tunnel wall. The observed values decreased approximately linearly with distance whereas the predicted varied asymptotically. The asymptotic distribution implies that all stress and strain changes occur in a very narrow zone around the tunnel. This is consistent with treating a continuum as being elastic. For example the stress distribution beneath a square footing decreases asymptotically with most of the stress change occuring within the depth of two footing widths (Sowers, 1970). In the case of tunnels, Terzaghi (1943) states that "At elevations of more than 5B (two and a half tunnel widths) above the centerline, the lowering of the strip seems to have no effect at all on the state of stress...." Thus according to elastic theory only a narrow zone in the vicinity of the boundary load is affected.

Other tunnel projects besides the one analysed here have indicated that deformations extend far beyond the tunnel wall

(Rowe and Kack, 1983). Consequently the validity of using models utilising elastic theory (linear and nonlinear) is questionable. It may very well be that creep models or elastic-plastic models provide better approximations of soil deformation in the vicinity of a tunnel. As a matter of fact according to the model used in this study a few elements were in a state of failure, implying a zero shear modulus and a small finite value had to be assigned to each of these elements to prevent a non-operative situation. However the computed deformations were not appreciably affected by these few elements. The occurrence of a plastic state in some elements suggests that the use of an elastic-plastic model might be more appropriate. The use of other models was beyond the scope of this study.

CONCLUSIONS

This practicum has investigated the applicability of a nonlinear load-deformation finite element program for estimating deformations associated with soft ground tunnelling in Winnipeg. Based on the results of the investigation, the following conclusions have been drawn.

1. The finite element method can be a very powerful tool when used correctly and its limitations are understood.
2. The bulk modulus of each element remained essentially constant for the entire stress change range.
3. The shear modulus underwent large changes (up to 100%) with stress changes in the soil indicating that the nonlinearity is primarily due to shear deformations.
4. There was very good agreement between the predicted deformations at the tunnel wall and the observed.
5. Agreement between the predicted and observed deformations beyond the tunnel wall were poor. The observed deformations decreased linearly with distance whereas the predicted approached zero asymptotically.

RECOMMENDATIONS

Based on the results of this investigation, the following recommendations have been suggested.

1. A future topic for study could be to investigate if tunnel deformations respond better to a creep model in which K & G = f(t).
2. A compilation of all pertinent data from existing case histories could be obtained so that design charts or curves similar to Peck et al may be developed for use in Winnipeg.
3. A future study to establish the long term earth pressures around the tunnel in Winnipeg clay or till would also be useful.

REFERENCES

Baracos, A., 1961. "The Stability of River Banks in the Metropolitan Winnipeg Area", Proc. 14th Can. Soil Mech. Conf. NRC. Technical Mem. No. 69.

Clough and Schmidt, 1981. "Soft Clay Engineering", Elsevier Scientific Publishing Company, Chapter 8.

Desai, C. S., 1968. "Solution of Stress Deformation Problems in Soil and Rock Mechanics using Finite Element Methods", Ph.D. Thesis, University of Texas, Austin.

Desai, C. S., Abel, J. F., 1972. "Introduction to the Finite Element Method", Van Nostrand Reinhold Company, N. Y.

Desai, C. S., Christian, J. T., 1977. "Numerical Methods in Geotechnical Engineering, McGraw-Hill, New York, N. Y.

Domaschuk, L., Valliappan, P., 1974. "Nonlinear Stress-Deformation Analyses of Lake Agassiz Clays Using Finite Element Methods", Geotechnical Research Series, Report No. 10.

Ghaboussi, J., Ranken, R. E., and Karshenas, M., 1978. "Analysis of Subsidence Over Soft-Ground Tunnels", Proc. Intl. Conf. on Evaluation and Prediction of Subsidence, ASCE, Pensacola Beach, Florida.

Graham, J., Houlsby, G. T., 1982. "Elastic Anisotrophy of a Natural Clay", Currently unpublished.

Hardy Assoc. Ltd. and R. V. Anderson Assoc. Ltd., 1981. "Tunnel Instrumentation Project, Year 1 Report".

Henkel, D. J., 1970. "Geotechnical Considerations of Lateral Stresses". Proc. Spec. Conf. Lateral Stresses in the Ground and Design of Earth Retaining Structures, Ithaca, N. Y.

Hoyaux and Ladanyi, 1970. "Gravitational Stress Field Around a Tunnel in Soft Ground", CGJ, Volume 7.

McAndrew, A. D., 1981. "A Study of Elastic Settlements using Finite Element Methods", Graduation Thesis, University of Manitoba.

Muir Wood, 1975. "The Circular Tunnel in Elastic Ground", Geotechnique, Volume 25.

Peck, R. B. 1969. "Deep Excavations and Tunnelling in Soft Ground", Proc. 7th Intl. Conf. on Soil Mechanics and Foundation Engineering, Mexico City.

Peck et al, 1972. "State of the Art of Soft Ground Tunnelling", Proc. N. American Rapid Excavation and Tunnelling Conf., Chicago, Ill.

Rowe, R. K. and Kack, G. J., 1983. "Some Applications for Analysis in the Estimating of Surface Settlements Caused by Tunnelling in Soft Ground", CGJ, Volume 20.

Rowe, R. K., Lo, K. Y. and Kack, G. J., 1983. "A Method of Estimating Surface Settlements Above Shallow Tunnels in Soft Soil", CGJ, Volume 20.

Sowers, G. B. and Sowers, G. F., 1970. "Introductory Soil Mechanics and Foundations", The MacMillan Company, New York, N. Y.

Tan and Clough, 1980. "Ground Control for Shallow Tunnels by Soil Grouting", Jour. of the Geotechnical Engineering Division, ASCE, Volume 106.

Terzaghi, K., 1943. "Theoretical Soil Mechanics", John Wiley and Sons, Inc. New York, N. Y.

Yong, E. O. F., 1983. "Creep Behaviour of Frozen Saline Silt Under Isotropic Compression", University of Manitoba, Master of Science Graduation Thesis.

Zienkiewicz, O. C., 1971. "The Finite Element Method in Engineering Science", McGraw Hill, London.

APPENDIX A

Chapter IV of Domaschuk and Valliappan (1974) describes the specific testing details and the complete bulk modulus derivation. The following is a brief summary of that chapter.

The results of the isotropic compression tests clearly indicated the stress-strain relationship was nonlinear. As shown in Figure 17, the increase in volumetric strain (ε_v) decreased with increasing isotropic stress (σ_m). They also found, the bulk modulus behaved differently above and below the preconsolidation pressure (Pc'). Above Pc', in the normally consolidated region, the bulk modulus varied linearly with stress level. Below Pc', in the overconsolidated region, the bulk modulus remained nearly constant.

The isotropic compression results also indicated that soil type (as defined by its plastic limit) affected the rate of change of ε_v and σ_m. Specifically, soils having low plastic indecies (P.I.) underwent less volume change than those with higher P.I.'s (for the same initial void ratio (e_o) and isotropic stress (σ_m)) as shown in Figure 18.

In the program developed by Domaschuk and Valliappan (1974), a three parameter relationship was chosen to represent the isotropic stress-strain behaviour observed in the laboratory. The basic equation was given by:

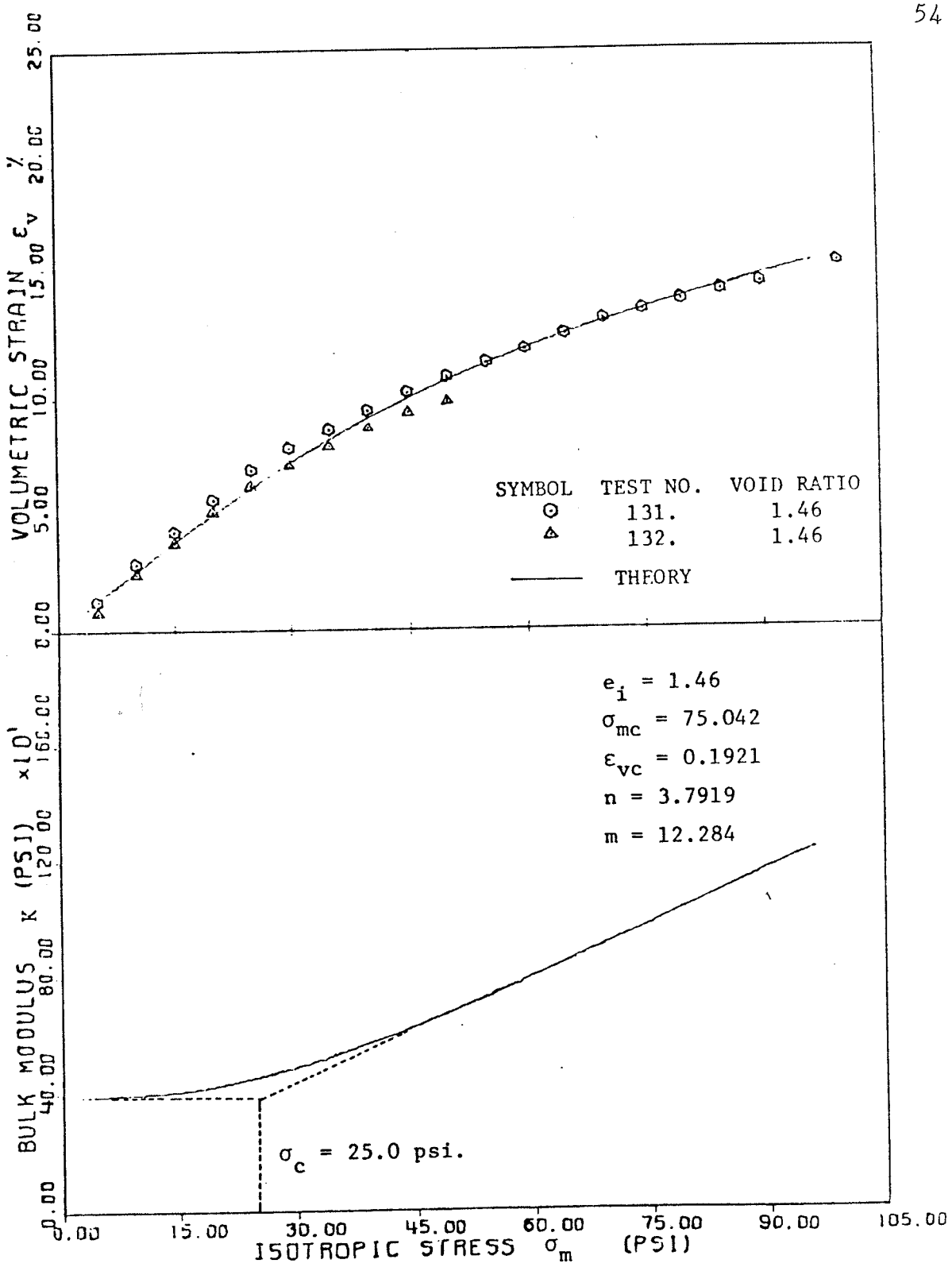

Figure 4.3. Isotropic Stress-Strain Curve and Solution for Bulk Modulus; Series No. 13.

Figure 17: After Domaschuk and Valliappan (1974)

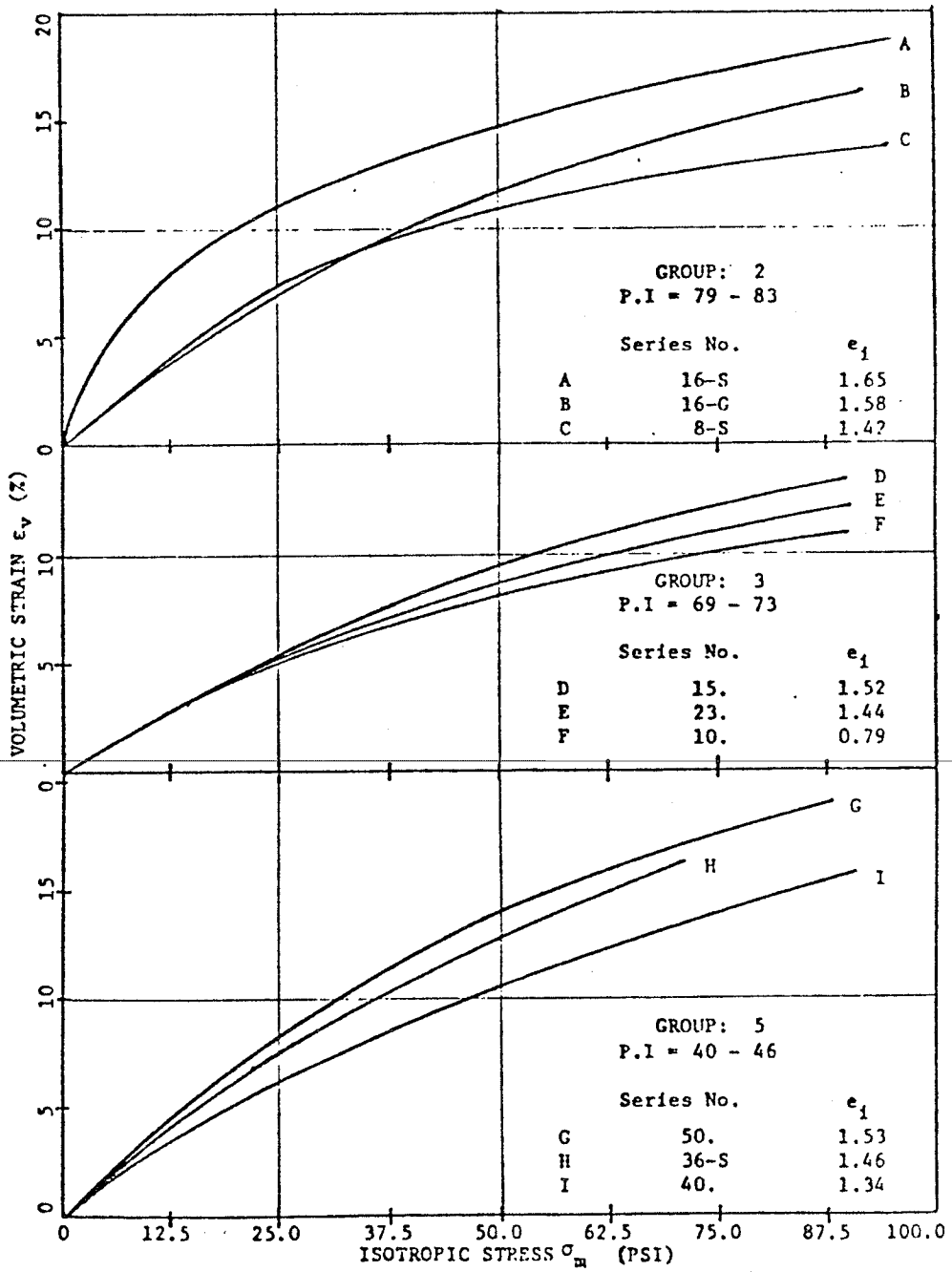

Figure 4.6. Typical Grouping of Isotropic Stress-Strain Data According to Atterberg Limits.

Figure 18: After Domaschuk and Valliappan (1974)

$$\frac{\sigma_m}{\sigma_{mc}} = \frac{\varepsilon_v}{\varepsilon_{vc}} \left\{1 + \left|\frac{\varepsilon_v}{\varepsilon_{vc}}\right|^{n-1}\right\} \qquad \text{(A1)}$$

where σ_m & ε_v = isotropic stress and strain respectively

σ_{mc} & ε_{vc} = characteristic values of isotropic stress and strain respectively

n = shape parameter

The values of σ_{mc}, ε_{vc}, and n for each material type were evaluated by the method of least squares to obtain a best fit solution. Knowing the value of σ_m, it is possible to solve for ε_v using Newton's method of iteration.

The solution for the bulk modulus was then obtained simply by differentiating equation A1 with respect to ε_v yielding:

$$\frac{d\sigma_m}{d\varepsilon_v} = K = \frac{\sigma_{mc}}{\varepsilon_{vc}} \left\{1 + n \left|\frac{\varepsilon_v}{\varepsilon_{vc}}\right|^{n-1}\right\} \qquad \text{(A2)}$$

where $\frac{\sigma_{mc}}{\varepsilon_{vc}}$ = the initial bulk modulus

Equation A2 was then used directly in the finite element program.

APPENDIX B

Chapter V of Domaschuk and Valliappan (1974) describes the specific testing details and the complete shear modulus (G) derivation. The following is a brief summary of that chapter.

The results of the constant-mean-normal triaxial tests clearly indicated a nonlinear relationship existed between the principal stress difference ($\sigma_1 - \sigma_3$) and axial strain (ε_1). As shown in Figures 19 to 21, the rate of change of ($\sigma_1 - \sigma_3$) decreased with increasing axial strains.

The plots of volume strain (ε_v) vs axial strain (ε_1), also shown in Figures 19 to 21, indicated the volume change was a function of the 'reduced' overconsolidation ratio ($\frac{\sigma_m}{P_c'}$). The samples with ratios less than 0.6 exhibited positive dilatency (i.e. - expansion), while those with ratios greater than 0.6 exhibited negative dilatency.

Domaschuk and Valliappan chose to use a hyperbolic relationship to describe the resultant deviatoric stress (S_d) vs resultant deviatoric strain (ε_d) behaviour for various reduced overconsolidation ratios. Due to the poorly defined final portion of the curve, a failure ratio (R_f), defined as the observed failure stress to the asymptotic value of the model, was determined statistically for each test, the average result was $R_f = 0.82$.

Log - log plots of the resultant deviatoric stress at

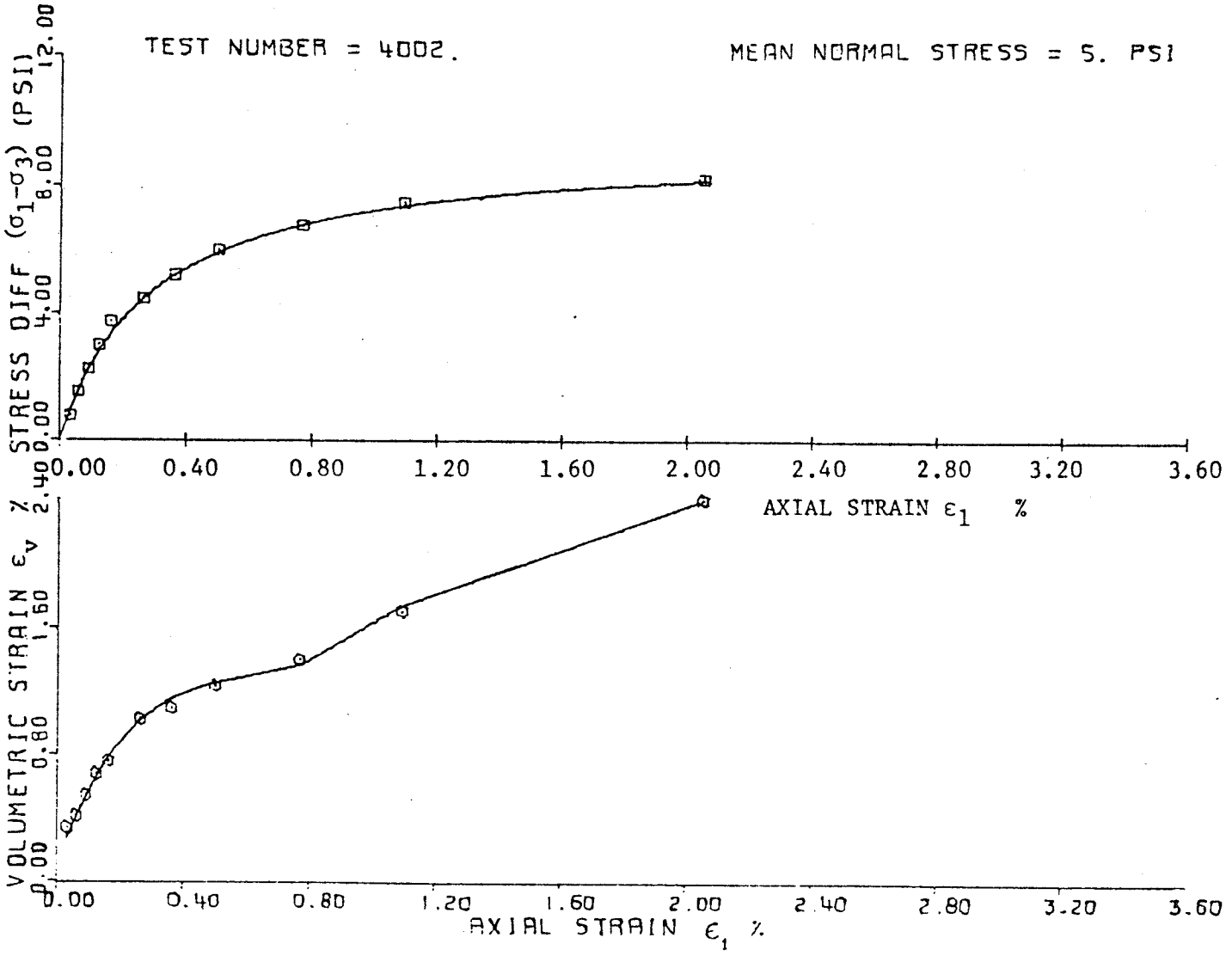

Figure 5.9. Principal Stress Difference and Volumetric Strain as Functions of Axial Strain for Constant $\frac{\sigma_m}{\sigma_c}$ = 0.2; Depth 40 ft.

Figure 19: After Domaschuk and Valliappan (1974)

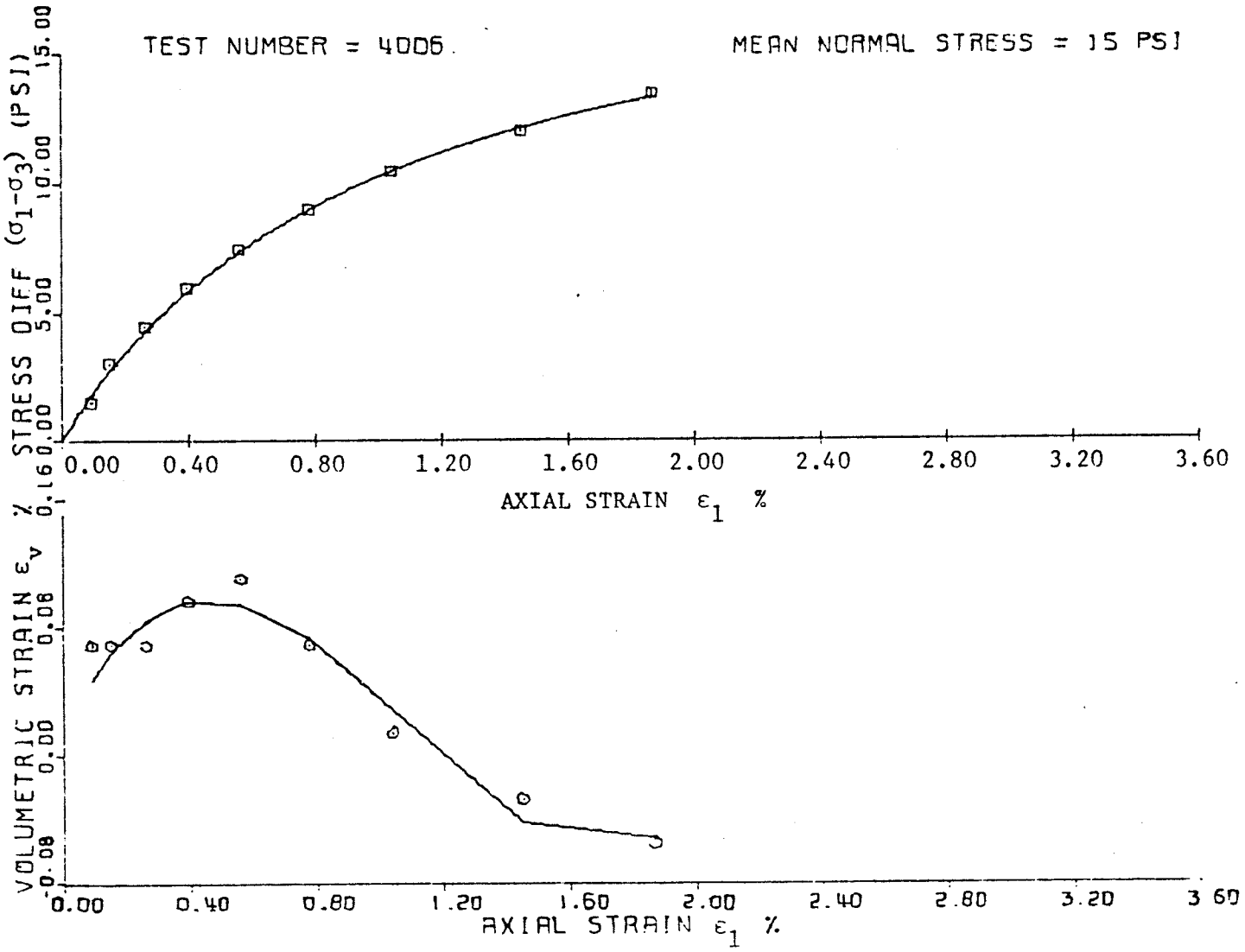

Figure 5.7. Principal Stress Difference and Volumetric Strain as Functions of Axial Strain for Constant $\frac{\sigma_m}{\sigma_c}$ = 0.6; Depth 40 ft.

Figure 20: After Domaschuk and Valliappan (1974)

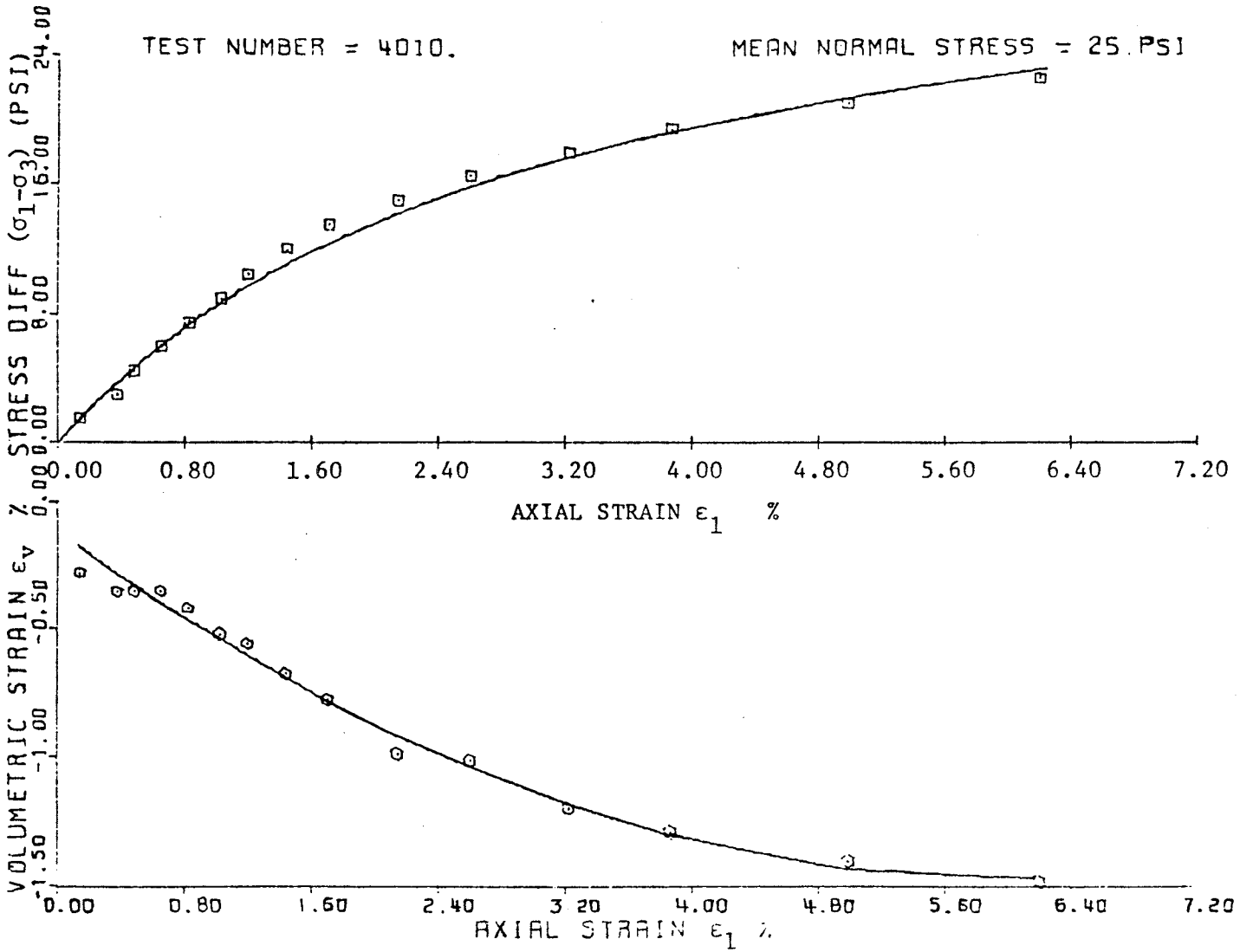

Figure 5.5. Principal Stress Difference and Volumetric Strain as Functions of Axial Strain for Constant $\frac{\sigma_m}{\sigma_c}$ = 1.0; Depth 40 ft.

Figure 21: After Domaschuk and Valliappan (1974)

failure (S_{df}) with a normalised variable, defined by $\frac{\sigma_m}{P'_c e_o}$, clearly indicated a linear relationship existed, from which the following failure criterion was obtained:

$$S_{df} = 10^{\alpha\{\frac{\sigma_m}{P'_c e_o}\}^{\beta}} \qquad (B.1)$$

in which S_{df} = resultant deviatoric stress at failure

P'_c = preconsolidation pressure

σ_m = effective-mean-normal stress

e_o = initial void ratio

α & β = linear regression coefficients in log - log plotting, referred to as failure criterion parameters

Comparing the individual failure criterions for the brown and blue clays it was apparent that they behaved differently. As shown in Figures 22 and 23, the resultant deviatoric stress at failure (S_{df}) decreased with increase in plasticity index (for any given $\frac{\sigma_m}{P'_c e_o}$ ratio) for the brown clays. The opposite was true for the blue clays.

In the program developed by Domaschuk and Valliappan, the resultant deviatoric stress-strain curve was given by:

$$S_d = \frac{\varepsilon_d G_o}{1 + b\varepsilon_d G_o} \qquad (B.2)$$

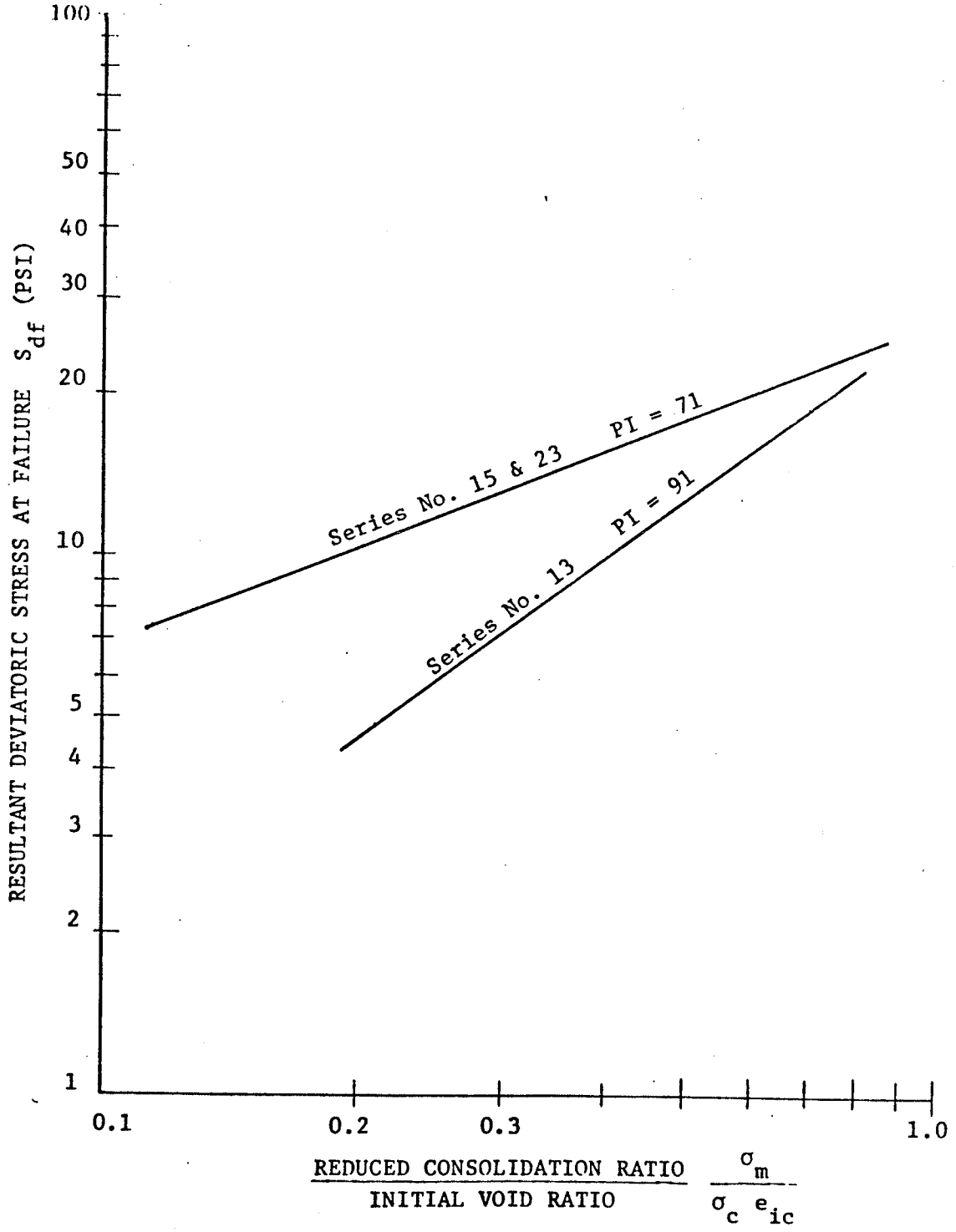

Figure 5.18. Failure Criterion Relationships for Brown Clays.

Figure 22: After Domaschuk and Valliappan (1974)

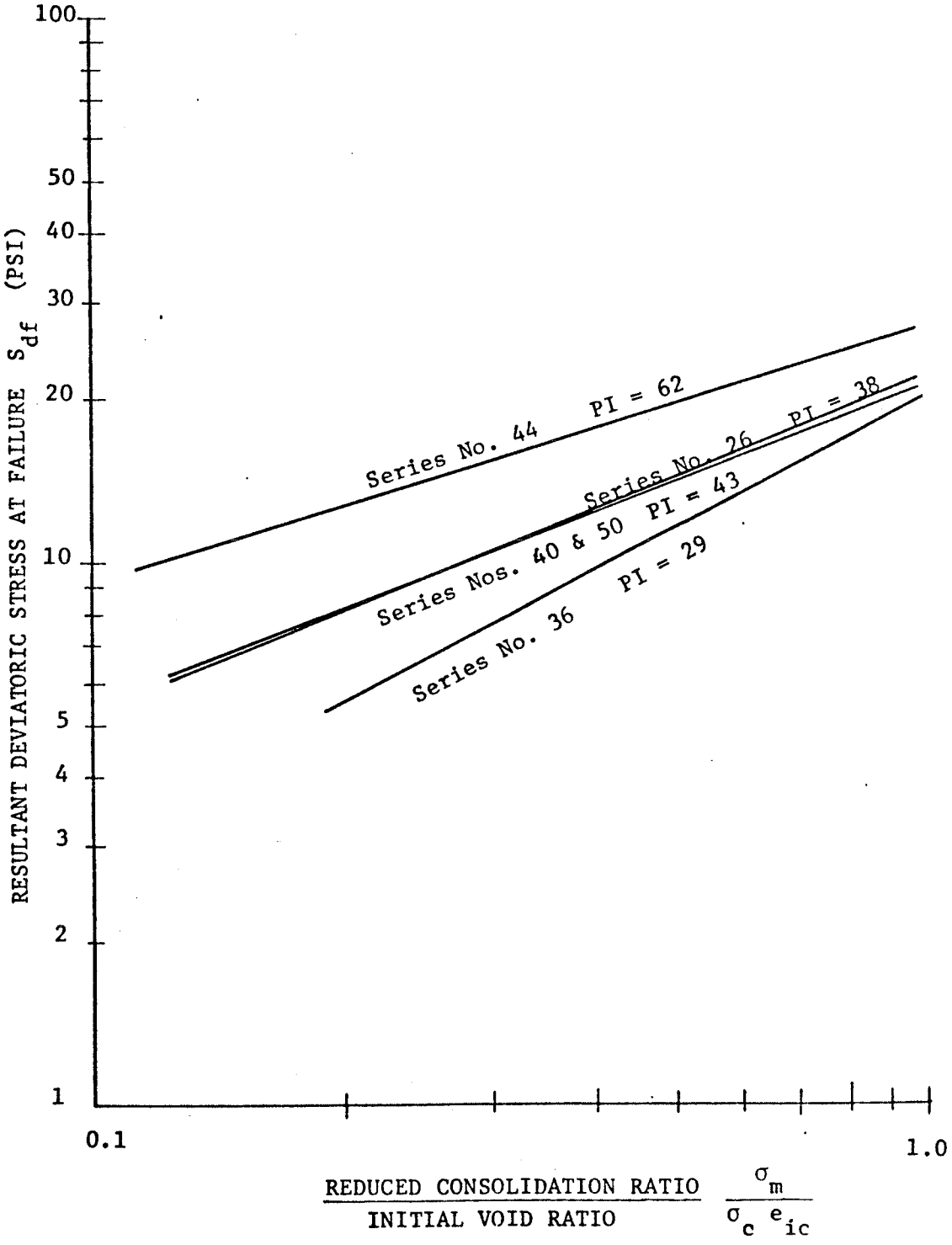

Figure 5.19. Failure Criterion Relationships for Blue Clays.

Figure 23: After Domaschuk and Valliappan (1974)

where S_d & ε_d = the resultant deviatoric stress and strain respectively

G_o = initial tangent modulus

b = reciprocal of the asymptotic value of the resultant deviatoric stress

Investigating the effect of initial void ratio and the ratio of mean normal stress to the preconsolidation pressure on the initial tangent modulus (G_o) was done by combining the variables $\frac{G_o}{\sigma_m}$ and $\frac{\sigma_m}{P'_c e_o}$. The variation of log $\frac{G_o}{\sigma_m}$ with $\frac{\sigma_m}{P'_c e_o}$ indicated a linear relationship existed in the form:

$$\text{Log}_{10}\left(\frac{G_o}{\sigma_m}\right) = A - B\left(\frac{\sigma_m}{P'_c e_o}\right) \qquad (B.3)$$

where A & B = semilogarithmic regression coefficients

Rewriting equation B.3 gave the general solution:

$$G_o = \sigma_m * 10^{\{A - B(\frac{\sigma_m}{P'_c e_o})\}} \qquad (B.4)$$

A linear regression analysis of equation B.4 indicated that for the brown clays, located at depths above 23 feet, A and B were constant, being equal to 2.3286780 and 1.1157590 respectively. Below 23 feet, in the blue clays, only B was considered a constant, being equal to 0.8114248. The coefficient A, on the other hand, was expressed as a function of the plastic index and given

by:

$$A = \frac{10^C}{(PI)^D} \tag{B.5}$$

where C & D = regression coefficients given by 0.88573 and 0.348 respectively

Differentiating equation B.2 with respect to ε_d gave:

$$\frac{dS_d}{d\varepsilon_d} = G = G_o(1 - bS_d)^2 \tag{B.6}$$

As explained earlier, the asymptotic value was related to the observed resultant deviatoric stress at failure by the failure ratio, R_f:

$$S_{df} = R_f * S_{dult} = R_f * \frac{1}{b} \tag{B.7}$$

Expressing the value of S_{df} in terms of the failure criterion, defined by equation B.1, equation B.7 was rewritten as:

$$b = \frac{R_f}{S_{df}} = \frac{R_f}{10^{\alpha\{\frac{\sigma_m}{P'_c e_o}\}^\beta}} \tag{B.8}$$

Substituting for b, equation B.4 became:

$$G = G_o\{1 - R_f(\frac{S_d}{10^{\alpha\{\frac{\sigma_m}{P'_c e_o}\}^\beta}})\}^2 \tag{B.9}$$

which was used directly in the finite element program.

APPENDIX C

The Displacement Method involves introducing a function that will approximate the element displacements at each node. The displacement model chosen depends on two factors; first, the accuracy required, and second, the degrees of freedom associated with each node. In this program, a very simple model has been used (linear) which corresponds to the two degrees of freedom as each node (i.e. - the displacements in the X & Y directions), and is given by:

$$\{u\} = [\Phi]\{\alpha\} \tag{C.1}$$

where $\{u\}$ = vector of displacement at any point within the element

$[\Phi]$ = generalized coordinate model

$\{\alpha\}$ = vector of generalized displacements

For the three node elements used in this case (referred to as constant strain triangles), equation (C.1) becomes:

$$\{q\} = [A]\{\alpha\} \tag{C.2}$$

where $\{q\} = \begin{Bmatrix} u_i \\ u_j \\ u_k \\ v_i \\ v_j \\ v_k \end{Bmatrix}$ $\quad [A] = \begin{bmatrix} 1 & x & y & 0 & 0 & 0 \\ 1 & x & y & 0 & 0 & 0 \\ 1 & x & y & 0 & 0 & 0 \\ 0 & 0 & 0 & 1 & x & y \\ 0 & 0 & 0 & 1 & x & y \\ 0 & 0 & 0 & 1 & x & y \end{bmatrix}$

$$\text{or} \quad \{\alpha\} = [A]^{-1}\{q\} \tag{C.3}$$

where $[A]^{-1}$ = displacement transformation matrix

$\{q\}$ = vector of nodal displacements

From equations (C.1) and (C.3) it follows that:

$$\{u\} = [\Phi][A]^{-1}\{q\} \tag{C.4}$$

which represents displacements at any point (x,y) within the element in terms of nodal displacements {q}.

The element displacements and strains are related by applying the theory of elasticity as follows:

$$\varepsilon_x = \frac{du}{dx} = \alpha_2 \qquad \varepsilon_y = \frac{dv}{dy} = \alpha_6$$

$$\gamma_{xy} = \frac{du}{dy} + \frac{dv}{dx} = \alpha_3 + \alpha_5$$

from which

$$\{\varepsilon\} = [B_\alpha]\{\alpha\} \tag{C.5}$$

where $[B_\alpha] = \begin{bmatrix} 0 & 1 & 0 & 0 & 0 & 0 \\ 0 & 0 & 0 & 0 & 0 & 1 \\ 0 & 0 & 1 & 0 & 1 & 0 \end{bmatrix}$ $\{\alpha\} = \begin{Bmatrix} \alpha_1 \\ \alpha_2 \\ \alpha_3 \\ \alpha_4 \\ \alpha_5 \\ \alpha_6 \end{Bmatrix}$

$\{\varepsilon\} = \begin{Bmatrix} \varepsilon_x \\ \varepsilon_y \\ \gamma_{xy} \end{Bmatrix}$

Substituting equation (C.3) into (C.5):

$$\{\varepsilon\} = [B_\alpha][A]^{-1}\{q\} \tag{C.6}$$

$$\text{or} \quad \{\varepsilon\} = [B]\{q\} \tag{C.7}$$

where $\{\varepsilon\}$ = vector of strains at any point within the element

$[B_\alpha]$ = strain displacement matrix for generalized coordinates

[B] = strain displacement matrix for interpolation models

The general stress-strain relationship for a plane strain case, in terms of the bulk and shear moduli (K & G) can be expressed as:

$$\{\sigma\} = [C]\{\varepsilon\} \tag{C.8}$$

where $[C] = \begin{bmatrix} K + 4G/3 & K + 2G/3 & 0 \\ K + 2G/3 & K + 4G/3 & 0 \\ 0 & 0 & G \end{bmatrix}$ $\{\sigma\} = \begin{Bmatrix} \sigma_x \\ \sigma_y \\ \tau_{xy} \end{Bmatrix}$

in which [C] = stress-strain matrix, which depends entirely on the material properties

$\{\sigma\}$ = vector of stresses at any point within the element

Combining equations (C.7) and (C.8), the following relationship develops:

$$\{\sigma\} = [C][B]\{q\} \tag{C.9}$$

The element stiffness matrix and load vector can be formulated by using the principle of virtual displacements, which states that the external work done on the body (Q) must equal the internal work done on the stresses in the body (W). The element stiffness is determined by equating the work quantities. The internal work is given by:

$$\{W_i\} = \int_{vol} \{\varepsilon\}^T\{\sigma\}\, dV \tag{C.10}$$

while the external work is given by:

$$\{Q\} = \int_{vol} \{w\}^T \{X\}\, dV + \iint_{area} \{w\}^T \{T\}\, dA \qquad (C.11)$$

where $\{X\}$ = vector of known body force intensities

$\{T\}$ = vector of known surface traction intensities

By applying the appropriate variational principles many of the terms vanish, leaving only:

$$\{Q\} = [k]\{q\} \qquad (C.12)$$

where $$[k] = \int_{vol} [B]^T [C] [B]\, dV \qquad (C.13)$$

For plane strain elements the volume integral is simply the area of the element, as its depth is always unity. This implies the element stiffness is given by:

$$[k] = A[B]^T [C] [B] \qquad (C.14)$$

where A = element area